

BI-TP 2006/26  
 FTUV-06-0720  
 IFIC/06-18  
 hep-lat/0607027

## Probing the chiral weak Hamiltonian at finite volumes

P. Hernández<sup>a,1</sup> and M. Laine<sup>b,2</sup>

<sup>a</sup>*Dpto. Física Teórica and IFIC, Edificio Institutos Investigación,  
 Apt. 22085, E-46071 Valencia, Spain*

<sup>b</sup>*Faculty of Physics, University of Bielefeld, D-33501 Bielefeld, Germany*

### Abstract

Non-leptonic kaon decays are often described through an effective chiral weak Hamiltonian, whose couplings (“low-energy constants”) encode all non-perturbative QCD physics. It has recently been suggested that these low-energy constants could be determined at finite volumes by matching the non-perturbatively measured three-point correlation functions between the weak Hamiltonian and two left-handed flavour currents, to analytic predictions following from chiral perturbation theory. Here we complete the analytic side in two respects: by inspecting how small (“ $\epsilon$ -regime”) and intermediate or large (“ $p$ -regime”) quark masses connect to each other, and by including in the discussion the two leading  $\Delta I = 1/2$  operators. We show that the  $\epsilon$ -regime offers a straightforward strategy for disentangling the coefficients of the  $\Delta I = 1/2$  operators, and that in the  $p$ -regime finite-volume effects are significant in these observables once the pseudoscalar mass  $M$  and the box length  $L$  are in the regime  $ML \lesssim 5.0$ .

July 2006

---

<sup>1</sup>pilar.hernandez@ific.uv.es

<sup>2</sup>laine@physik.uni-bielefeld.de

## 1. Introduction

Understanding why the  $\Delta I = 1/2$  amplitudes for non-leptonic kaon decays are so much larger than the  $\Delta I = 3/2$  amplitudes, is a long-standing problem for QCD phenomenology. It has been known since the early 70s that the bulk of the enhancement must be due to strong interactions at low energies [1]. Therefore a reliable explanation must eventually be based on systematic non-perturbative methods, in particular on lattice QCD [2, 3].

It was realized long ago that instead of computing directly the decay amplitudes with lattice QCD, a simpler alternative is to use lattice simulations to determine the relevant low-energy constants (LECs) of the effective chiral weak Hamiltonian that describes kaon decays [3], and then use chiral perturbation theory to compute the physical amplitudes [3]–[8]. The determination of the LECs can be achieved by matching certain observables computed in lattice QCD and in chiral perturbation theory ( $\chi$ PT), as close as possible to the chiral limit. In this respect it is advantageous to approach the chiral limit by first extrapolating to small or zero quark masses, and increase the volume only afterwards. This setup corresponds to the so-called  $\epsilon$ -regime of  $\chi$ PT [9] (see also Ref. [10]). The power-counting rules in this regime [9] guarantee that the contamination from higher order LECs is reduced very significantly. In other words, the number of LECs that appear at the next-to-leading order (NLO) in the  $\epsilon$ -regime of  $\chi$ PT is typically much smaller than that at the next-to-leading order in the standard  $p$ -regime, where the infrared cutoff is provided by the pion mass rather than the volume.

The matching of lattice QCD and the chiral effective theory in the  $\epsilon$ -regime has recently been considered in order to extract the strong interaction LECs [11]–[18]. Subsequently, it has been pursued for the determination of the weak LECs that we are interested in [15, 19, 20], as well as for the study of baryon properties [21]. This progress has been possible thanks to the advent of Ginsparg-Wilson formulations of lattice fermions [22]–[29], which possess an exact chiral symmetry in the limit of vanishing quark masses. Simulations in this regime are however challenging on the numerical side, and Refs. [15, 17] introduced several important technical advances in order to make them possible.

In Ref. [20], a strategy based on these methods has been proposed to reveal the role that the charm quark mass plays in the  $\Delta I = 1/2$  rule. In particular, following the suggestion of Ref. [15], the observables that are considered are three-point correlation functions of two left-handed flavour currents and the weak operators. The first step is the matching of these observables, to extract the LECs of the weak chiral effective Hamiltonian, in a theory with a light charm quark, that is in a four-flavour theory with an exact  $SU(4)$  symmetry in the valence sector. The results of this computation can be found in Ref. [30]. The next step of the strategy is to increase the charm quark mass and monitor the LECs as we move towards a theory with an  $SU(3)$  flavour symmetry [20, 31].

In a previous paper [19], we have already computed the NLO  $\epsilon$ -regime predictions for the correlators of left-handed flavour currents and the  $\Delta I = 3/2$  weak operator, whose coefficient determines the kaon mixing parameter  $\hat{B}_K$  in the chiral limit. The purpose of the present

paper is to extend the results of Ref. [19] in two ways. First of all, we compute the same observables as before, but also at larger quark masses, corresponding to the  $p$ -regime of chiral perturbation theory. The goal is to obtain a better understanding of the regions of validity of the  $\epsilon$  and  $p$ -regimes. Second, we include the  $\Delta I = 1/2$  weak operators in the analysis.

We find that the  $\epsilon$ -regime does offer a clean way of disentangling the coefficients of the two leading-order  $\Delta I = 1/2$  operators.

It is well known that the description of quenched simulations, which still are widely in use today, through a quenched version of chiral perturbation theory, is rather problematic. In particular the  $p$ -regime is strongly affected by quenched ambiguities that increase significantly the number of LECs [32], making it difficult to identify those that should be closest to the ones in the full theory. We have studied the effect of these ambiguities also in the  $\epsilon$ -regime at NLO, and find that they are significantly less severe in this case.

In most of our analysis we will concentrate, however, on the full physical theory. The most immediate applications might then follow through the use of mixed fermion frameworks [33], though progress towards dynamical Ginsparg-Wilson fermions is also taking place [34].

It should be made clear from the onset that choosing to consider correlators involving left-handed flavour currents in this paper, is not meant to indicate that they would necessarily be the ultimate way for determining the weak LECs. For instance, employing the zero-mode wave functions of the massless Dirac operator might also lead to a useful probe, even though for the pion decay constant they seem to be slightly disfavoured in comparison with the left-handed flavour currents [16].

Other methods to obtain the weak LECs have also been considered in the literature. For lattice approaches without an exact chiral invariance see, e.g., the recent work in Refs. [35]. For models inspired by the large- $N_c$  expansion see, e.g., Refs. [36, 37].

This paper is organised as follows. We formulate the problem in Sec. 2, discuss the various regimes of chiral perturbation theory in Sec. 3, address the  $\Delta I = 3/2$  operators in Sec. 4, and the  $\Delta I = 1/2$  operators in Sec. 5. We conclude in Sec. 6.

## 2. Formulation of the problem

We start by considering QCD with 4 flavours. The quark part of the Euclidean continuum Lagrangian reads

$$L_E = \sum_{r=1}^4 \bar{\psi}_r (\gamma_\mu D_\mu + m_r) \psi_r , \quad (2.1)$$

where  $r$  is a flavour index; the Dirac matrices  $\gamma_\mu$  are assumed normalised such that  $\gamma_\mu^\dagger = \gamma_\mu$ ,  $\{\gamma_\mu, \gamma_\nu\} = 2\delta_{\mu\nu}$ ;  $D_\mu$  is the covariant derivative;  $m_r$  is the quark mass; colour and spinor indices are assumed contracted; and repeated indices are summed over, even when no summation symbol is shown explicitly. In the following we will consider the three lightest quarks as degenerate in mass,  $m_u = m_d = m_s \equiv m$ , while the charm quark is heavier,  $m_c \gg m$ .

After an operator product expansion in the inverse W boson mass, weak interactions can be described with the Fermi theory involving four-quark operators. In the CP conserving case of two generations, the effective weak Hamiltonian is then [1] (for reviews see, e.g., [38, 39])

$$H_w = 2\sqrt{2}G_F V_{ud} V_{us}^* \left\{ \sum_{\sigma=\pm 1} h_w^\sigma \left( [O_w]_{suud}^\sigma - [O_w]_{sccd}^\sigma \right) + h_m [O_m]_{sd} \right\} + \text{H.c.} , \quad (2.2)$$

where  $h_w^\pm, h_m$  are scheme-dependent dimensionless Wilson coefficients, with leading order values  $h_w^\pm = 1, h_m = 0$ . The coefficients  $h_w^\pm$  are known to two loops in perturbation theory [40], while  $h_m$  remain undetermined. In Eq. (2.2) we have introduced the notation

$$[O_w]_{rsuv}^\sigma \equiv \frac{1}{2} \left( [O_w]_{rsuv} + \sigma [O_w]_{rsvu} \right) , \quad (2.3)$$

$$[O_w]_{rsuv} \equiv (\bar{\psi}_r \gamma_\mu P_- \psi_u) (\bar{\psi}_s \gamma_\mu P_- \psi_v) , \quad (2.4)$$

$$[O_m]_{sd} \equiv (m_c^2 - m_u^2) \{ m_s (\bar{\psi}_s P_- \psi_d) + m_d (\bar{\psi}_s P_+ \psi_d) \} . \quad (2.5)$$

Here  $r, s, u, v$  are generic flavour indices, while  $u, d, s, c$  denote the physical flavours. The chiral projection operators  $P_\pm$  read  $P_\pm \equiv (1 \pm \gamma_5)/2$ , where  $\gamma_5 = \gamma_0 \gamma_1 \gamma_2 \gamma_3$ . The colour and spinor indices are assumed to be contracted within the parentheses.

In order to match the Hamiltonian of Eq. (2.2) to the one in the SU(3) chiral theory, the first step is to decompose it into irreducible representations of the  $SU(3)_L \times SU(3)_R$  flavour group, present at low energies. The weak operators are singlets under  $SU(3)_R$ , and projecting them onto irreducible representations of  $SU(3)_L$ , the weak Hamiltonian can be rewritten as

$$H_w = 2\sqrt{2}G_F V_{ud} V_{us}^* \left\{ h_w^+ [\hat{O}_w]_{suud}^+ + \frac{1}{5} h_w^+ [R_w]_{sd}^+ - h_w^- [R_w]_{sd}^- - \frac{1}{2} (h_w^+ + h_w^-) [O_w]_{sccd} - \frac{1}{2} (h_w^+ - h_w^-) [O_w]_{scdc} + h_m [O_m]_{sd} \right\} + \text{H.c.} , \quad (2.6)$$

where

$$[\hat{O}_w]_{suud}^+ \equiv \frac{1}{2} \left\{ [O_w]_{suud} + [O_w]_{sudu} - \frac{1}{5} \sum_{k=u,d,s} \left( [O_w]_{skdk} + [O_w]_{skkd} \right) \right\} , \quad (2.7)$$

$$[R_w]_{sd}^\pm \equiv \frac{1}{2} \sum_{k=u,d,s} \left( [O_w]_{skdk} \pm [O_w]_{skkd} \right) . \quad (2.8)$$

The first operator in Eq. (2.6) transforms under the 27-plet of the  $SU(3)_L$  subgroup: it is symmetric under the interchange of quark or antiquark indices, and traceless. The remaining ones, transforming as  $\mathbf{3}^* \otimes \mathbf{3}$  and being traceless, belong to irreducible representations of dimension 8.

If, as the next step, the charm quark is also integrated out, then the operators in Eq. (2.6) go over into the standard ones, commonly denoted by  $Q_i$ ,  $i = 1, \dots, 6$  [41, 42] (of which five

are independent). It is probably safer to keep the charm quark in the simulations, though, since integrating it out perturbatively is not guaranteed to be a safe procedure. Moreover, the quenched three-flavour theory contains spurious operators [32]. For these reasons, we prefer to consider the four-flavour theory of Eq. (2.6) to be the QCD-side of our problem.

Now, at large distances, the physics of QCD can be reproduced by chiral perturbation theory. For a degenerate quark mass matrix, the leading order chiral Lagrangian reads

$$\mathcal{L}_{\chi\text{PT}} = \frac{F^2}{4}\text{Tr}\left[\partial_\mu U \partial_\mu U^\dagger\right] - \frac{m\Sigma}{2}\text{Tr}\left[e^{i\theta/N_f} U + U^\dagger e^{-i\theta/N_f}\right], \quad (2.9)$$

where  $U \in \text{SU}(N_f)$ ,  $N_f \equiv 3$ , and  $\theta$  is the vacuum angle. Apart from  $\theta$ , this Lagrangian contains two parameters, the pseudoscalar decay constant  $F$  and the chiral condensate  $\Sigma$ . At the next-to-leading order in the momentum expansion, additional operators appear in the chiral Lagrangian, with the associated low-energy constants  $L_1, L_2, \dots$  [43].

Obviously the chiral model can be extended to include a weak Hamiltonian [44]. We denote the chiral analogue of  $H_w$  in Eq. (2.6) by  $\mathcal{H}_w$ . To again define dimensionless coefficients, we write  $\mathcal{H}_w$  in the form [3, 5]

$$\mathcal{H}_w \equiv 2\sqrt{2}G_F V_{ud} V_{us}^* \left\{ \frac{5}{3}g_{27}\mathcal{O}_{27} + 2g_8\mathcal{O}_8 + 2g'_8\mathcal{O}'_8 \right\} + \text{H.c.} , \quad (2.10)$$

where  $g_{27}, g_8$  and  $g'_8$  are the low-energy constants we are interested in. The operators read

$$\mathcal{O}_{27} \equiv [\hat{\mathcal{O}}_w]_{suud}^+ = \frac{3}{5}\left([\mathcal{O}_w]_{sudu} + \frac{2}{3}[\mathcal{O}_w]_{suud}\right), \quad (2.11)$$

$$[\mathcal{O}_w]_{rsuv} \equiv \frac{F^4}{4}\left(\partial_\mu U U^\dagger\right)_{ur}\left(\partial_\mu U U^\dagger\right)_{vs}, \quad (2.12)$$

$$\mathcal{O}_8 \equiv [\mathcal{R}_w]_{sd}^+ = \frac{1}{2} \sum_{k=u,d,s} [\mathcal{O}_w]_{skkd}, \quad (2.13)$$

$$\mathcal{O}'_8 \equiv \frac{F^2}{2}m\Sigma\left(e^{i\theta/N_f} U + U^\dagger e^{-i\theta/N_f}\right)_{ds}, \quad (2.14)$$

where we have made use of  $\text{Tr}[\partial_\mu U U^\dagger] = 0$  to simplify the chiral versions of Eqs. (2.7), (2.8).

In the following, we will find it useful to generalize the notation somewhat from the standard  $\text{SU}(3)$  case introduced above. Let  $N_v \equiv 3$  be the number of valence flavours, and  $N_f$  the number of degenerate sea flavours in the chiral Lagrangian. The standard case corresponds to  $N_f = N_v$ , but one can also envisage other interesting situations, for instance  $N_f = 4$  [20], or  $N_f \rightarrow 0$ . We note that the simplified forms in Eqs. (2.11), (2.13) only apply for  $N_f = N_v$ ; in general, the combinations in Eqs. (2.7), (2.8) need to be employed (the generalizations of these combinations to arbitrary  $N_v, N_f$  are summarised in Appendix A). In the remainder of this Section we have in mind the case  $N_f = N_v$  but the formulae are written in a way which will be useful in Appendix C, where we analyse the situation  $N_f \neq N_v$ .

The principal strategy now is to construct three-point functions by correlating  $H_w$  with two left-handed flavour currents on the QCD side, and to match to predictions from  $\chi\text{PT}$  for

the same objects. In QCD, the left-handed flavour current can formally be defined as

$$J_\mu^a \equiv \bar{\psi} T^a \gamma_\mu P_- \psi , \quad (2.15)$$

where  $T^a$  is a traceless generator of the valence group  $SU(N_v)$ , and all colour, flavour, and spinor indices are assumed contracted. Note that  $J_\mu^a$  defined this way is formally purely imaginary.<sup>3</sup>

The two and three-point correlation functions between the left-handed currents and the weak operators, averaged over the spatial volume, now read [15]:

$$\text{Tr} [T^a T^b] C(x_0) \equiv \int d^3x \left\langle J_0^a(x) J_0^b(0) \right\rangle , \quad (2.16)$$

$$[C_R]^{ab}(x_0, y_0) \equiv \int d^3x \int d^3y \left\langle J_0^a(x) O_R(0) J_0^b(y) \right\rangle , \quad (2.17)$$

where the index  $R$  refers to the representation.

On the  $\chi$ PT side, the operator corresponding to Eq. (2.15) becomes, at leading order in the momentum expansion,

$$\mathcal{J}_\mu^a = \frac{F^2}{2} \text{Tr} \left[ T^a U \partial_\mu U^\dagger \right] . \quad (2.18)$$

The two-point correlation function  $\mathcal{C}(x_0)$  is defined (apart from contact terms) by

$$\text{Tr} [T^a T^b] \mathcal{C}(x_0) = \int d^3x \left\langle \mathcal{J}_0^a(x) \mathcal{J}_0^b(0) \right\rangle , \quad (2.19)$$

and the three-point correlation function we are interested in, reads (again apart from contact terms)

$$[\mathcal{C}_R]^{ab}(x_0, y_0) \equiv \int d^3x \int d^3y \left\langle \mathcal{J}_0^a(x) \mathcal{O}_R(0) \mathcal{J}_0^b(y) \right\rangle . \quad (2.20)$$

Our task is to compute the objects in Eqs. (2.19), (2.20) under certain circumstances, to be specified in the next Section.

### 3. Regimes of chiral perturbation theory

Given a fixed spatial extent  $L \gg 1/F$  of the box, several different kinematical regimes can be identified in  $\chi$ PT, leading to various computational procedures [45]. The situation is summarised in Fig. 1. We will here be interested in the  $p$ - and  $\epsilon$ -regimes; the  $\delta$ -regime (corresponding to small but elongated boxes) is also relevant in principle, but quite tedious to handle in practice [45], and thus preferably avoided.

<sup>3</sup>The convention in Eq. (2.15) differs by a factor  $i$  from that in Ref. [19], but agrees with the convention of Refs. [17, 20]. We use this “unphysical” convention since it removes a number of unnecessary overall minus signs from the  $\chi$ PT predictions.

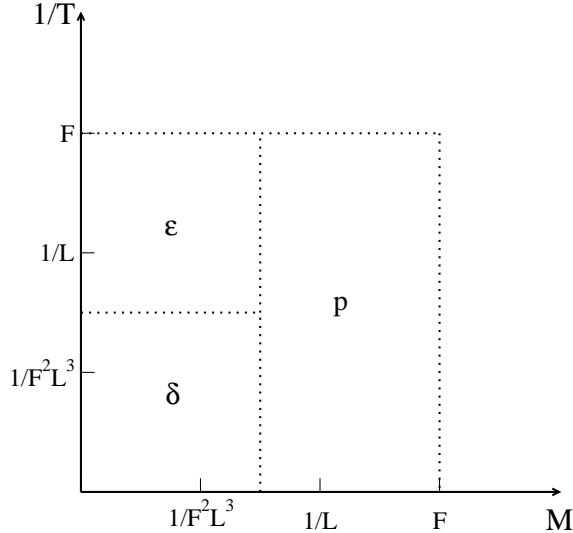


Figure 1: The different regimes of chiral perturbation theory, given a fixed spatial extent  $L$  of the box, according to Ref. [45]. Here  $T$  is the temporal extent of the box and  $M$  the pseudoscalar mass. It is assumed that  $L \gg 1/F$ .

### 3.1. $p$ -regime

In the  $p$ -regime, we express the outcome as a power series in  $M^2/F^2$ , where  $M^2 \equiv 2m\Sigma/F^2$  is the pseudoscalar mass. The power-counting rules for the  $p$ -regime are that

$$M \sim p, \quad L \gtrsim \frac{1}{p}, \quad (3.1)$$

where  $p$  is assumed a small quantity,  $p \ll F$ . The temporal extent  $T$  can in principle be small or large, as long as  $T \gtrsim 1/p$ . It follows from these assignments that the Goldstone field  $\xi$ , defined through  $U = \exp(2i\xi/F)$ , behaves effectively as a small quantity, and can be expanded in.

Inserting the Taylor-series of  $U$  into Eq. (2.9), the propagator becomes

$$\langle \xi_{ur}(x) \xi_{vs}(y) \rangle = \frac{1}{2} \left[ \delta_{us} \delta_{vr} G(x - y; M^2) - \delta_{ur} \delta_{vs} E(x - y; M^2) \right], \quad (3.2)$$

where

$$G(x; M^2) = \frac{1}{V} \sum_{n \in \mathbb{Z}^4} \frac{e^{ip \cdot x}}{p^2 + M^2}, \quad p \equiv (p_0, \mathbf{p}) \equiv 2\pi \left( \frac{n_0}{T}, \frac{\mathbf{n}}{L} \right), \quad (3.3)$$

and  $V \equiv TL^3$  is the volume. Here we have also set  $\theta = 0$ , as is usually done in the  $p$ -regime. In the unquenched case,  $E(x; M^2) = G(x; M^2)/N_f$ , but we keep everywhere  $E(x; M^2)$  completely general. The reason is that then the form of Eq. (3.2) is general enough to contain also the propagator of the replica formulation of quenched chiral perturbation theory [46, 13].

For future reference and as an example of a NLO result in the  $p$ -regime, we consider the two-point correlation function in Eq. (2.19). The result can be written as

$$\begin{aligned}\mathcal{C}(x_0) &= \frac{F^2}{2} \left\{ \left[ 1 - \frac{N_f G(0; M^2)}{F^2} + \frac{8M^2}{F^2} (N_f L_4 + L_5) \right] M^2 P(x_0) - \frac{N_f}{F^2} \frac{dG(0; M^2)}{dT} \right. \\ &+ \left. \left[ \frac{E(0; M^2)}{F^2} - \frac{8M^2}{F^2} (N_f L_4 + L_5 - 2N_f L_6 - 2L_8) \right] M^2 \frac{d}{dM^2} [M^2 P(x_0)] \right\},\end{aligned}\quad (3.4)$$

where (for  $|x_0| \leq T$ )

$$P(x_0) \equiv \int d^3 \mathbf{x} G(x; M^2) = \frac{1}{T} \sum_{p_0} \frac{e^{ip_0 x_0}}{p_0^2 + M^2} = \frac{\cosh[M(T/2 - |x_0|)]}{2M \sinh[MT/2]}, \quad (3.5)$$

while

$$G(0; M^2) \equiv G_\infty(M^2) + G_V(M^2), \quad (3.6)$$

where  $G_\infty(M^2)$  is the infinite-volume value,<sup>4</sup>

$$G_\infty(M^2) \equiv \int \frac{d^d p}{(2\pi)^d} \frac{1}{p^2 + M^2}, \quad (3.7)$$

and the (finite) function  $G_V(M^2)$  incorporates all the volume dependence [47],<sup>5</sup>

$$G_V(M^2) = \frac{1}{(4\pi)^2} \int_0^\infty \frac{d\lambda}{\lambda^2} e^{-\lambda M^2} \sum_{n \in \mathbb{Z}^4} \left( 1 - \delta_{n,0}^{(4)} \right) \exp \left[ -\frac{1}{4\lambda} \left( T^2 n_0^2 + L^2 |\mathbf{n}|^2 \right) \right]. \quad (3.8)$$

For  $MV^{\frac{1}{4}} \gg 1$ , the finite-volume effects are exponentially small, and we can set  $G_V = 0$ .

### 3.2. $\epsilon$ -regime

In the  $\epsilon$ -regime, the natural dimensionless variable is  $\mu \equiv m\Sigma V$ . The power counting rules are

$$m\Sigma \lesssim \epsilon^4, \quad L \sim \frac{1}{\epsilon}, \quad T \sim \frac{1}{\epsilon}, \quad (3.9)$$

where  $\epsilon$  is assumed small,  $\epsilon \ll F$ . Hence the parameter  $\mu$  is parametrically of up to order unity. In this regime, the Goldstone boson zero-mode  $U_0$ , defined by writing  $U = \exp(2i\bar{\xi}/F)U_0$ , where  $\bar{\xi}$  has non-zero momenta only, dominates the dynamics, and needs to be treated non-perturbatively. Consequently, gauge field topology plays an important role [48], and it is useful to give the predictions in sectors of a fixed topological charge  $\nu$ .

As an example, the two-point correlation function  $\mathcal{C}(x_0)$  of Eq. (2.19) becomes [49, 14, 19]

$$\mathcal{C}(x_0) = \frac{F^2}{2T} \left[ 1 + \frac{N_f}{F^2} \left( \frac{\beta_1}{\sqrt{V}} - \frac{T^2 k_{00}}{V} \right) + \frac{2T^2 \mu}{F^2 V} \sigma_\nu(\mu) h_1(\hat{x}_0) \right], \quad (3.10)$$

<sup>4</sup>The divergence of  $G_\infty(M^2)$  for  $d \approx 4$  cancels against those in the  $L_i$ 's [43], cf. Eqs. (B.17), (B.31).

<sup>5</sup>In Ref. [47] the function  $G_V$  was denoted by  $g_1$ .

where  $\hat{x}_0 \equiv x_0/T$ , and the constants  $\beta_1$  and  $k_{00}$  are related to the (dimensionally regularised) value of

$$\bar{G}(x) \equiv \frac{1}{V} \sum_{n \in \mathbb{Z}^4} \left(1 - \delta_{n,0}^{(4)}\right) \frac{e^{ip \cdot x}}{p^2}, \quad (3.11)$$

by

$$\bar{G}(0) \equiv -\frac{\beta_1}{\sqrt{V}}, \quad T \frac{d}{dT} \bar{G}(0) \equiv \frac{T^2 k_{00}}{V}. \quad (3.12)$$

Introducing  $\rho \equiv T/L$  and

$$\hat{\alpha}_p(l_0, l_i) \equiv \int_0^1 dt t^{p-1} \left[ S(l_0^2/t) S^3(l_i^2/t) - 1 \right], \quad (3.13)$$

where  $S(x)$  is an elliptic theta-function,  $S(x) = \sum_{n=-\infty}^{\infty} \exp(-\pi x n^2) = \vartheta_3(0, \exp(-\pi x))$ , a numerical evaluation of these coefficients is allowed by (see, e.g., Refs. [47, 49])

$$\beta_1 = \frac{1}{4\pi} \left[ 2 - \hat{\alpha}_{-1} \left( \rho^{\frac{3}{4}}, \rho^{-\frac{1}{4}} \right) - \hat{\alpha}_{-1} \left( \rho^{-\frac{3}{4}}, \rho^{\frac{1}{4}} \right) \right], \quad (3.14)$$

$$k_{00} = \frac{1}{12} - \frac{1}{4} \sum_{\mathbf{n} \neq 0} \frac{1}{\sinh^2(\pi \rho |\mathbf{n}|)}. \quad (3.15)$$

Furthermore,  $\sigma_\nu(\mu) \equiv N_f^{-1} d\{\ln \det[I_{\nu+j-i}(\mu)]\}/d\mu$ , where the determinant is taken over an  $N_f \times N_f$  matrix, whose matrix element  $(i, j)$  is the modified Bessel function  $I_{\nu+j-i}$  [50, 48]. The function  $h_1(\tau)$  appearing in Eq. (3.10) reads (for  $|\tau| \leq 1$ )

$$h_1(\tau) \equiv \frac{1}{2} \left[ \left( |\tau| - \frac{1}{2} \right)^2 - \frac{1}{12} \right]. \quad (3.16)$$

### 3.3. Further remarks

In the following, we carry out computations according to the  $p$  and  $\epsilon$ -countings as outlined above. Other recent work for related observables has made use of the  $p$ -regime, with  $T \gg L$  [51, 52, 53]. There have also been extensive NLO computations at infinite volume [54], which is a special limit of the  $p$ -regime.

Note that if  $1/FL \ll 1$  as our power-counting rules assume, and we consider an observable that is independent of the topological charge  $\nu$ , then the  $\epsilon$  and  $p$ -regimes should in principle be continuously connected to each other (cf. Fig. 1). Concretely, for  $ML \ll 1$  and  $T \sim L$ , Eq. (3.4) goes over into Eq. (3.10) with  $\mu \gg 1$ , in which limit the dependence of Eq. (3.10) on  $\nu$  disappears. Whether such a crossover takes place in practice remains to be inspected for each observable separately, and gives some feeling concerning the convergence of the  $\chi$ PT computation, i.e., whether  $1/FL \ll 1$  is satisfied.

## 4. The $\Delta I = 3/2$ operator

We now address the determination of  $g_{27}$ , considered previously in the  $\epsilon$ -regime [19].

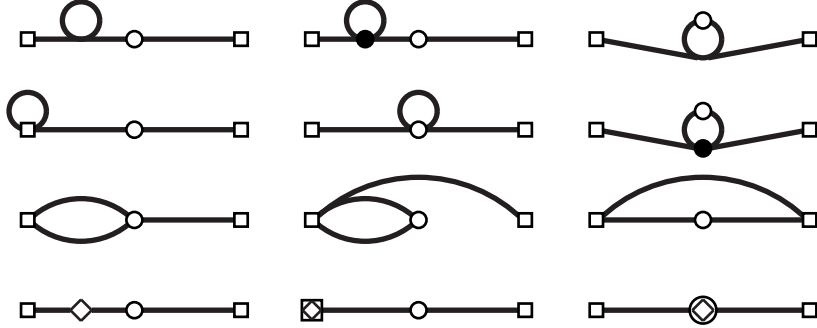


Figure 2: The NLO graphs for  $\mathcal{C}_{27}$  in the  $p$ -regime. Lines denote meson propagators, an open square the left-handed current, an open circle the weak operator, and a closed circle a four-point interaction emerging from the “mass term” in the chiral Lagrangian. Diamonds indicate QCD and weak interaction  $O(p^4)$  low-energy constants.

#### 4.1. $p$ -regime

The graphs entering the computation of Eq. (2.20) at next-to-leading relative order in the  $p$ -regime are shown in Fig. 2, with the weak operator  $\mathcal{O}_{27}$  to be taken from Eq. (2.11). The result can be written in the form

$$[\mathcal{C}_{27}]^{ab}(x_0, y_0) = \Delta_{27}^{ab} \left[ \mathcal{C}(x_0)\mathcal{C}(y_0) + \mathcal{D}_{27}(x_0, y_0) \right], \quad (4.1)$$

where (for  $N_v = 3$ )

$$\Delta_{27}^{ab} = \frac{3}{5} T_{ds}^{\{a} T_{uu}^{b\}} + \frac{2}{5} T_{us}^{\{a} T_{du}^{b\}}. \quad (4.2)$$

As an example, choosing kaon and pion type currents, we could take

$$T_{ij}^a \equiv \delta_{iu} \delta_{js} \Leftrightarrow J_0^a = \bar{u} \gamma_0 P_- s, \quad (4.3)$$

$$T_{ij}^b \equiv \delta_{id} \delta_{ju} \Leftrightarrow J_0^b = \bar{d} \gamma_0 P_- u, \quad (4.4)$$

and then

$$\Delta_{27}^{ab} = \frac{2}{5}. \quad (4.5)$$

Given the result for  $\mathcal{C}(x_0)$  in Eq. (3.4), the only further missing ingredient in Eq. (4.1) is  $\mathcal{D}_{27}(x_0, y_0)$ . We obtain

$$\begin{aligned} \mathcal{D}_{27}(x_0, y_0) = & -\frac{F^2}{4} \left\{ \frac{M^2}{T} \frac{d^2 G(0; M^2)}{dT^2} + M^2 \frac{dG(0; M^2)}{dT} \left[ P(x_0) + P(y_0) \right] + \right. \\ & + 2M^4 G(0; M^2) P(x_0) P(y_0) - \frac{1}{2} M^4 P(x_0 - y_0) \left[ B(x_0) + B(y_0) \right] + \\ & \left. + M^4 \int_0^T d\tau P'(\tau - x_0) P'(\tau - y_0) B(\tau) \right\}, \end{aligned} \quad (4.6)$$

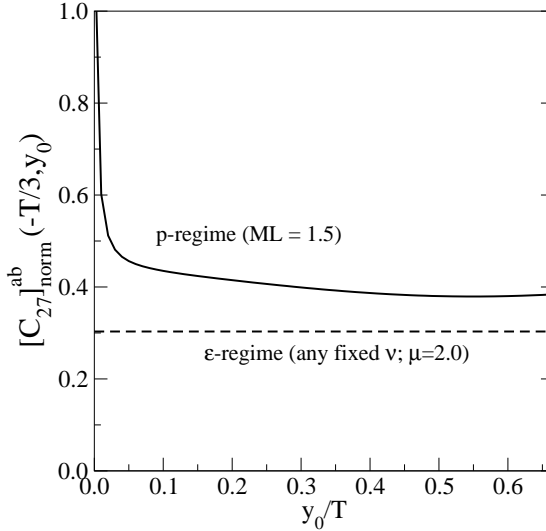


Figure 3: The function  $[\mathcal{C}_{27}]_{\text{norm}}^{ab}(-T/3, y_0)$ . The parameters are:  $N_f = 3$ ,  $F = 93$  MeV,  $L = 2$  fm,  $T/L = 2$ ,  $\Lambda = 1000$  MeV.

where the new object  $B(x_0)$  is defined as (for  $|x_0| < T$ )

$$B(x_0) = \int d^3\mathbf{x} \left[ G(x; M^2) \right]^2 = \frac{1}{L^3} \sum_{\mathbf{p}} \left[ \frac{\cosh[E(T/2 - |x_0|)]}{2E \sinh[ET/2]} \right]^2 \Big|_{E \equiv \sqrt{M^2 + \mathbf{p}^2}} . \quad (4.7)$$

The expression in Eq. (4.6) is, as such, ultraviolet divergent: in dimensional regularization in  $d = 4 - 2\epsilon$  dimensions, the third and the last terms on the right-hand side contain poles in  $\epsilon$ . Denoting  $\lambda \equiv -1/32\pi^2\epsilon$ , we can write

$$\mathcal{D}_{27}(x_0, y_0) = \mathcal{D}_{27}^r(x_0, y_0) + F^2 \lambda \left[ \frac{1}{2} M^4 P'(x_0) P'(y_0) - M^6 P(x_0) P(y_0) \right] , \quad (4.8)$$

where  $\mathcal{D}_{27}^r(x_0, y_0)$  is finite. The divergences get cancelled against the  $\mathcal{O}(p^4)$  low-energy constants related to weak interactions, as shown in Appendix B. As there are a large number of them, however, it is sufficient for our purposes here to note that the  $\mathcal{O}(p^4)$  low-energy constants amount to cancelling the  $1/\epsilon$ -divergences in the result and replacing the corresponding  $\overline{\text{MS}}$  scheme scale parameter  $\bar{\mu}$  by two different physical scales,  $\Lambda$  for the coefficient of  $P(x_0)P(y_0)$  and  $\Lambda'$  for the coefficient of  $P'(x_0)P'(y_0)$ .

For practical applications, it is convenient to normalise the three-point correlator by dividing with two two-point correlators:

$$[\mathcal{C}_{27}]_{\text{norm}}^{ab}(x_0, y_0) \equiv \frac{[\mathcal{C}_{27}]^{ab}(x_0, y_0)}{\mathcal{C}(x_0)\mathcal{C}(y_0)} = \Delta_{27}^{ab} \left[ 1 + \frac{\mathcal{D}_{27}(x_0, y_0)}{\mathcal{C}(x_0)\mathcal{C}(y_0)} \right] \equiv \Delta_{27}^{ab} \left[ 1 + \mathcal{R}_{27}(x_0, y_0) \right] . \quad (4.9)$$

The function  $\mathcal{R}_{27}(x_0, y_0)$  is then trivially obtained from Eqs. (4.6) and (3.4); in Eq. (3.4), it is even enough to keep the leading order contribution only, since  $\mathcal{D}_{27}(x_0, y_0)$  gets generated only at NLO.

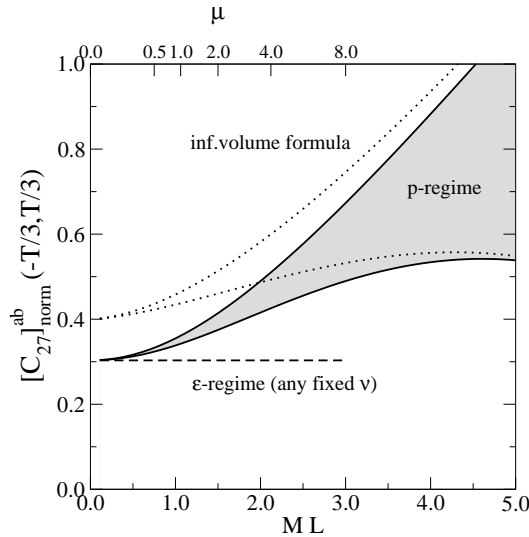


Figure 4: The values of  $[\mathcal{C}_{27}]_{\text{norm}}^{ab}(-T/3, T/3)$ . The parameters are:  $N_f = 3$ ,  $F = 93$  MeV,  $L = 2$  fm,  $T/L = 2$ ,  $\Lambda = (500 - 2000)$  MeV.

As an example, the function  $[\mathcal{C}_{27}]_{\text{norm}}^{ab}(-T/3, y_0)$  is plotted in Fig. 3 as a function of  $y_0$ , for the index choice in Eq. (4.5) (solid line). The values of  $[\mathcal{C}_{27}]_{\text{norm}}^{ab}(-T/3, T/3)$  are shown in Fig. 4, as a function of  $ML$  (the region bounded by solid lines). In these plots, the effects of the weak LECs have been collected to a single scale  $\Lambda = \Lambda'$  appearing inside the logarithms, and the scale has been varied in a wide range, to indicate the size of the uncertainty related to the unknown higher order LECs.

We would like to stress at this point that the  $p$ -regime results are parametrically valid only in the range  $ML \gtrsim 1/FL$ : for generic observables, the contributions of the Goldstone zero-modes become dominant if this inequality is not satisfied, and need to be resummed, leading to the rules of the  $\epsilon$ -regime. It turns out [20], however, that in the normalised observable  $[\mathcal{C}_{27}]_{\text{norm}}^{ab}(x_0, y_0)$  that we have considered here, the contributions from the Goldstone zero-modes cancel out at this order. Therefore the result can in fact formally be expanded as a Taylor-series in  $(ML)^2$ , with the zeroth order term agreeing with the result of the  $\epsilon$ -regime (see below). Still, one has to keep in mind that the Taylor-expanded result only needs to reproduce the correct mass dependence in the range  $ML \gtrsim 1/FL$ .

Let us finally briefly touch the conventional limit of large volumes. We assume  $x_0 = -|x_0|$ ,  $y_0 = |y_0|$ , such that the charges are on opposite sides of the operator. Then  $P(x_0) = \exp(-M|x_0|)/2M$  and  $P'(x_0)P'(y_0) = -M^2P(x_0)P(y_0)$ . In other words, the distinction disappears between the two structures getting contributions from the higher order LECs (cf. Eq. (4.8)), just as would happen if a partial integration could be carried out with respect to the position of the weak operator. Consequently, only a single combination of LECs appears,

and the corresponding effects can be collected into a single scale  $\Lambda$ . We obtain

$$\mathcal{R}_{27}(x_0, y_0) = \frac{M^2}{(4\pi F)^2} \left[ 3 \ln \frac{\Lambda^2}{M^2} + 2 - e^{-2M|x_0|} \phi(2M|x_0|) - e^{-2M|y_0|} \phi(2M|y_0|) \right], \quad (4.10)$$

where

$$\phi(x) \equiv \int_0^\infty dz z^{\frac{1}{2}} e^{-xz} \frac{\sqrt{2+z}}{1+z} \left[ \frac{1}{2+z} + \frac{1}{1+z} - 2 \right]. \quad (4.11)$$

The  $x_0$  and  $y_0$ -dependences in Eq. (4.10) are very small in practice. As seen in Fig. 4 (dotted line), one needs to go to volumes as large as  $ML \gtrsim 5$  in order for the simple infinite-volume approximation to be accurate for this observable.

#### 4.2. $\epsilon$ -regime

The  $\epsilon$ -regime results for  $\mathcal{D}_{27}(x_0, y_0)$  were derived in Ref. [19] but, for completeness and future reference, we briefly reinstate them here. For  $\mathcal{D}_{27}$  in Eq. (4.1) one obtains

$$\mathcal{D}_{27}(x_0, y_0) = -\frac{F^2}{2T^2} \left( 1 + T \frac{d}{dT} \right) \bar{G}(0), \quad (4.12)$$

and, using Eq. (3.12) as well as the leading-order part of Eq. (3.10), the ratio in Eq. (4.9) becomes

$$\mathcal{R}_{27}(x_0, y_0) = \frac{2}{(FL)^2} \left[ \rho^{-\frac{1}{2}} \beta_1 - \rho k_{00} \right], \quad (4.13)$$

where  $\rho = T/L$ . Note that this result is independent of the topological charge  $\nu$ , although computed in a fixed topological sector.

The  $\epsilon$ -regime prediction for the function  $[\mathcal{C}_{27}]_{\text{norm}}^{ab}(-T/3, y_0)$  is plotted in Fig. 3 as a function of  $y_0$ , for the index choice in Eq. (4.5) (dashed line). The values of  $[\mathcal{C}_{27}]_{\text{norm}}^{ab}(-T/3, T/3)$  are shown in Fig. 4, as a function of  $\mu$  (dashed line).

#### 4.3. Further remarks

Let us inspect Fig. 4, around the region  $ML \sim 1.5$ , or  $\mu \sim 2.0$ . Moving to smaller values of  $\mu$ , the  $\epsilon$ -regime becomes more accurate, while at larger  $ML$ , the  $p$ -regime should be the correct procedure. But which result represents better the truth at this intermediate point, where both countings are in principle parametrically applicable?

Let us note that for the semi-realistic parameters used in Fig. 4,  $1/FL \approx 1.1$ . Therefore, the parametric rules we have assumed are at best satisfied by a narrow margin. Consequently, higher order corrections in  $\chi$ PT can be important. In the absence of an explicit computation thereof, it remains to be inspected phenomenologically which of the predictions reproduces better the volume and mass dependences of the simulation results in this regime.

We end with a small remark on quenching. Employing the replica formulation [46, 13] of quenched chiral perturbation theory [55, 56], the only changes with respect to the unquenched situation are that we need to replace the propagator of Eq. (3.2) through

$$E(x; M^2) \equiv \frac{\alpha}{2N_c} G(x; M^2) + \frac{m_0^2 - \alpha M^2}{2N_c} H(x; M^2), \quad (4.14)$$

$$H(x; M^2) \equiv \frac{1}{V} \sum_{n \in \mathbb{Z}^4} \frac{e^{ip \cdot x}}{(p^2 + M^2)^2}, \quad (4.15)$$

where new parameters related to axial singlet field,  $m_0^2/2N_c, \alpha/2N_c$ , have been introduced; and take  $N_f \rightarrow 0$  at the end of the computation. Given that our results for  $[\mathcal{C}_{27}]_{\text{norm}}^{ab}(x_0, y_0)$  are completely independent of  $N_f$  and of the function  $E(x; M^2)$ , however, there is no change with respect to the unquenched theory for this observable [19].

## 5. The $\Delta I = 1/2$ operators

In the case of the  $\Delta I = 1/2$  transitions, two operators appear in Eq. (2.10), allowed by the symmetries. This means that if we have measured some correlation function on the QCD side, with an operator  $O_8$  transforming in the octet representation, then this is to be matched to a linear combination of correlation functions on the  $\chi$ PT side:

$$\int d^3x \int d^3y \left\langle J_0^a(x) h_8 O_8(0) J_0^b(y) \right\rangle \equiv g_8 [\mathcal{C}_8]^{ab}(x_0, y_0) + g'_8 [\mathcal{C}'_8]^{ab}(x_0, y_0), \quad (5.1)$$

where  $h_8$  is the Wilson coefficient, and  $g_8, g'_8$  are the partial contributions from  $h_8 O_8$  to the corresponding LECs. We thus have to consider two different classes of correlators on the  $\chi$ PT side, in order to be able to disentangle the coefficients of these operators.

### 5.1. $p$ -regime

For the operator  $O_8$  of Eq. (2.13), the graphs entering the computation of the correlation function in Eq. (2.20) are the same as in Fig. 2, and the correlation function has the same form as in Eq. (4.1):

$$[\mathcal{C}_8]^{ab}(x_0, y_0) \equiv \Delta_8^{ab} [\mathcal{C}(x_0) \mathcal{C}(y_0) + \mathcal{D}_8(x_0, y_0)], \quad (5.2)$$

where

$$\Delta_8^{ab} = \frac{1}{2} \{T^a, T^b\}_{ds}, \quad (5.3)$$

and the function  $\mathcal{C}(x_0)$  is still given by Eq. (3.4). For the matrices  $T^a, T^b$  in Eqs. (4.3), (4.4), the group theory factor evaluates to

$$\Delta_8^{ab} = \frac{1}{2}. \quad (5.4)$$

The function  $\mathcal{D}_8(x_0, y_0)$  reads

$$\begin{aligned} \mathcal{D}_8(x_0, y_0) &= -\frac{N_v}{2} \mathcal{D}_{27}(x_0, y_0) + \\ &+ F^2 M^2 \frac{N_v + 2}{8} \left\{ \left[ G(0; M^2) - 2E(0; M^2) \right] P'(x_0) P'(y_0) + \right. \\ &+ M^2 P(x_0 - y_0) \left[ \tilde{B}(x_0) + \tilde{B}(y_0) - \frac{1}{2} B(x_0) - \frac{1}{2} B(y_0) \right] + \\ &+ P'(x_0 - y_0) \left[ \tilde{B}'(y_0) + \tilde{B}_0(y_0) + \frac{1}{2} B'(x_0) - \tilde{B}'(x_0) - \tilde{B}_0(x_0) - \frac{1}{2} B'(y_0) \right] + \\ &\left. + M^2 \int_0^T d\tau \left[ M^2 B(\tau) - 2M^2 \tilde{B}(\tau) - \tilde{B}_{00}(\tau) \right] P(\tau - x_0) P(\tau - y_0) \right\}. \quad (5.5) \end{aligned}$$

The new objects appearing here are defined as

$$\tilde{B}(x_0) \equiv \int d^3x G(x; M^2) E(x; M^2), \quad (5.6)$$

$$\tilde{B}_0(x_0) \equiv \int d^3x \left[ \partial_0 G(x; M^2) E(x; M^2) - G(x; M^2) \partial_0 E(x; M^2) \right], \quad (5.7)$$

$$\tilde{B}_{00}(x_0) \equiv \int d^3x \left[ \partial_0^2 G(x; M^2) E(x; M^2) - G(x; M^2) \partial_0^2 E(x; M^2) \right]. \quad (5.8)$$

We recall that in the unquenched theory,  $E(x; M^2) = G(x; M^2)/N_f$ , and  $\tilde{B}(x_0)$  thus agrees with  $B(x_0)/N_f$  as defined through Eq. (4.7), while  $\tilde{B}_0(x_0)$ ,  $\tilde{B}_{00}(x_0)$  vanish.

Eq. (5.5) again contains divergences: in the unquenched theory,

$$\begin{aligned} \mathcal{D}_8(x_0, y_0) &= \mathcal{D}_8^r(x_0, y_0) + F^2 \lambda \left[ \left( \frac{1}{2} - \frac{N_v + 2}{2N_f} \right) M^4 P'(x_0) P'(y_0) + \right. \\ &\left. + \left( \frac{N_v - 2}{4} + \frac{N_v + 2}{2N_f} \right) M^6 P(x_0) P(y_0) \right], \quad (5.9) \end{aligned}$$

where  $\lambda \equiv -1/32\pi^2\epsilon$ , and  $\mathcal{D}_8^r(x_0, y_0)$  is finite. The cancellation of these divergences against the  $O(p^4)$  LECs is demonstrated in Appendix B.

Following Eq. (4.9), it is convenient to define a normalised correlation function by dividing with two current-current correlators, and we thus obtain

$$[\mathcal{C}_8]_{\text{norm}}^{ab}(x_0, y_0) \equiv \frac{[\mathcal{C}_8]^{ab}(x_0, y_0)}{\mathcal{C}(x_0) \mathcal{C}(y_0)} = \Delta_8^{ab} \left[ 1 + \mathcal{R}_8(x_0, y_0) \right]. \quad (5.10)$$

Again, it is enough to use the leading order forms for the functions  $\mathcal{C}(x_0)$ ,  $\mathcal{C}(y_0)$  in the definition of  $\mathcal{R}_8(x_0, y_0)$ , since  $\mathcal{D}_8(x_0, y_0)$  gets generated only at NLO.

In the infinite-volume limit, the distinction between the various types of divergences in Eq. (5.9) disappears, as before. Collecting the corresponding LECs to a single scale  $\Lambda$ , we obtain (in the unquenched case)

$$\mathcal{R}_8(x_0, y_0) = -\frac{N_v}{2} \mathcal{R}_{27}(x_0, y_0) + \frac{N_v + 2}{2} \left( 1 - \frac{2}{N_f} \right) \frac{M^2}{(4\pi F)^2} \left[ 2 \ln \frac{\Lambda^2}{M^2} + 1 + \right.$$

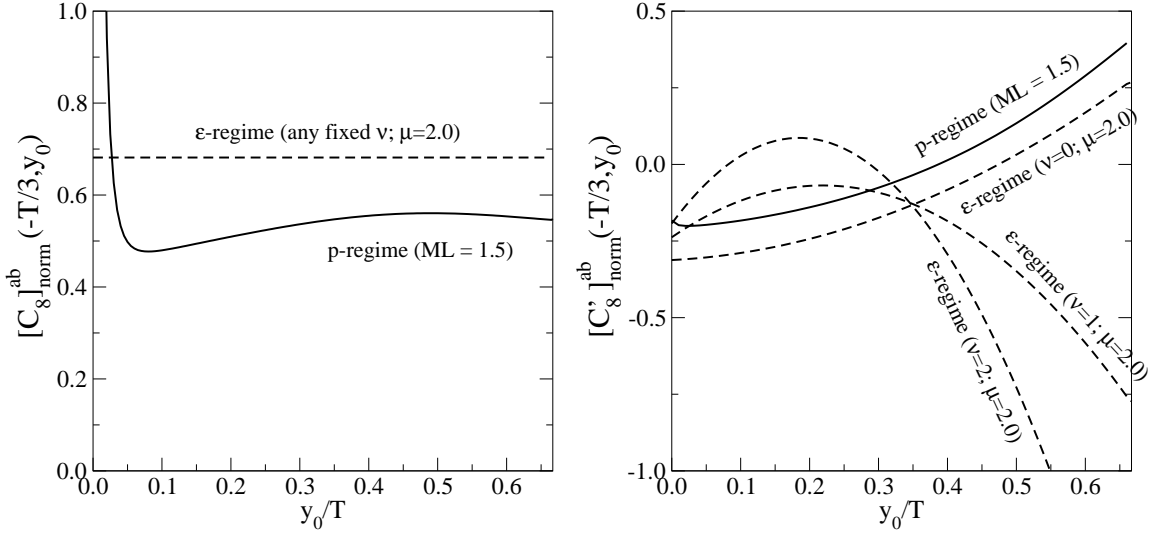


Figure 5: Left: the function  $[C_8]_{\text{norm}}^{ab}(-T/3, y_0)$ . Right: the function  $[C_8']_{\text{norm}}^{ab}(-T/3, y_0)$ . The parameters are:  $N_f = 3$ ,  $F = 93$  MeV,  $L = 2$  fm,  $T/L = 2$ ,  $\Lambda = 1000$  MeV.

$$+ e^{-2M|x_0|} \Xi(2M|x_0|) + e^{-2M|y_0|} \Xi(2M|y_0|) \Big] , \quad (5.11)$$

where  $\mathcal{R}_{27}(x_0, y_0)$  is from Eq. (4.10), and

$$\Xi(x) \equiv \int_0^\infty dz z^{\frac{1}{2}} e^{-xz} \frac{\sqrt{2+z}}{1+z} \left[ \frac{1}{2+z} - \frac{1}{1+z} + 2 + 4z \right] . \quad (5.12)$$

For the correlator  $C'_8$  the graphs are the same as in Fig. 2 except that, for a vacuum angle  $\theta = 0$ , the weak operator  $\mathcal{O}'_8$  only couples to an even number of Goldstone modes. The result is now of the form

$$[C'_8]^{ab}(x_0, y_0) \equiv \Delta_8^{ab} \mathcal{D}'_8(x_0, y_0) , \quad (5.13)$$

where

$$\begin{aligned} \mathcal{D}'_8(x_0, y_0) = & \frac{F^4}{2} \left\{ \left[ 1 - \frac{N_f G(0; M^2)}{F^2} + \frac{E(0; M^2)}{F^2} M^2 \frac{d}{dM^2} \right] \left[ M^2 P'(x_0) P'(y_0) \right] + \right. \\ & + \frac{N_f M^4}{2F^2} \int_0^T d\tau \left[ P'(\tau - x_0) P'(\tau - y_0) + M^2 P(\tau - x_0) P(\tau - y_0) \right] B(\tau) - \\ & \left. - \frac{2M^4}{F^2} \int_0^T d\tau P'(\tau - x_0) P'(\tau - y_0) \tilde{B}(\tau) - \frac{N_f}{2F^2} \frac{M^2}{T} \frac{dG(0; M^2)}{dM^2 dT} \right\} . \quad (5.14) \end{aligned}$$

Separating the divergent parts, we get (in the unquenched case)

$$\begin{aligned} \mathcal{D}'_8(x_0, y_0) = & \mathcal{D}'_8^r(x_0, y_0) + F^2 \lambda \left[ \left( -\frac{3N_f}{2} + \frac{3}{N_f} \right) M^4 P'(x_0) P'(y_0) - \frac{N_f}{2} M^6 P(x_0) P(y_0) + \right. \\ & \left. + \frac{1}{N_f} M^6 \frac{d}{dM^2} (P'(x_0) P'(y_0)) \right] , \quad (5.15) \end{aligned}$$

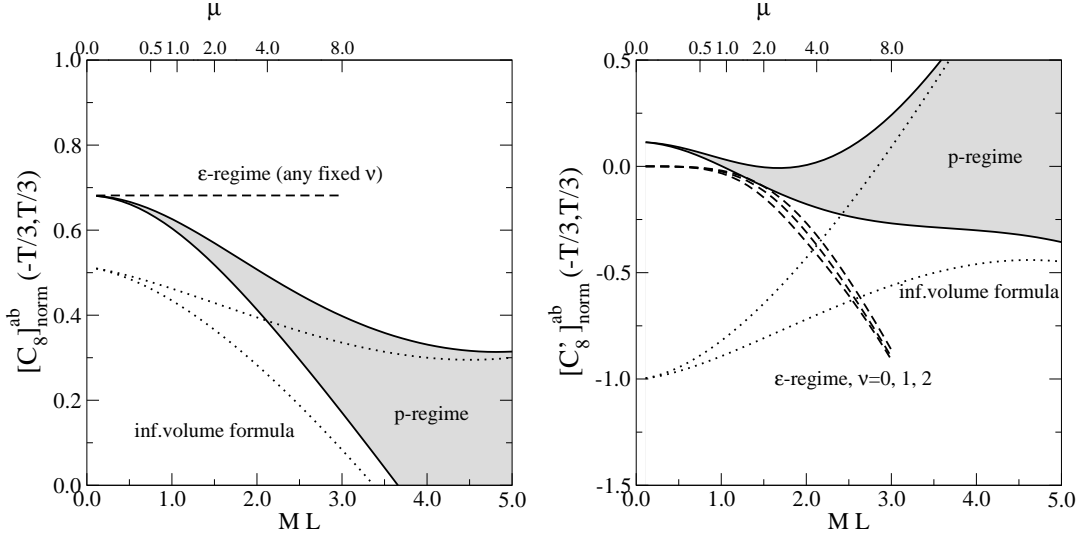


Figure 6: Left: the function  $[C_8]_{\text{norm}}^{ab}(-T/3, T/3)$ . Right: the function  $[C_8']_{\text{norm}}^{ab}(-T/3, T/3)$ . The parameters are:  $N_f = 3$ ,  $F = 93$  MeV,  $L = 2$  fm,  $T/L = 2$ ,  $\Lambda = (500 - 2000)$  MeV.

where  $\mathcal{D}_8'(x_0, y_0)$  is finite. The cancellation of divergences is demonstrated in Appendix B.

If we want to disentangle the dependences following from the operators  $\mathcal{O}_8$  and  $\mathcal{O}'_8$  in a given lattice measurement, we are lead to compare the contributions from  $\mathcal{O}'_8$  with the normalised correlation function in Eq. (5.10). Therefore, we define

$$[C_8']_{\text{norm}}^{ab}(x_0, y_0) \equiv \frac{[C_8']^{ab}(x_0, y_0)}{\mathcal{C}(x_0) \mathcal{C}(y_0)}. \quad (5.16)$$

Treating UV-divergences and higher order LECs as before, the correlation functions  $[C_8]_{\text{norm}}^{ab}(-T/3, y_0)$  and  $[C_8']_{\text{norm}}^{ab}(-T/3, y_0)$  are plotted in Fig. 5 as a function of  $y_0$  (solid lines). The two correlators are observed to have a rather different dependence on  $y_0$ , allowing in principle to disentangle their contributions in a given lattice measurement. The values of  $[C_8]_{\text{norm}}^{ab}(-T/3, T/3)$  and  $[C_8']_{\text{norm}}^{ab}(-T/3, T/3)$  as a function of  $ML$  are illustrated in Fig. 6 (regions bounded by solid lines).

It is important to stress that, for  $ML \rightarrow 0$ , the correction of relative order  $1/F^2$  in Eq. (5.14) diverges as  $\sim 1/F^2 M^2 V$ . This indicates in a concrete way that the  $p$ -regime computation is no longer reliable for  $ML \ll 1/FL$ , and we need to turn to the  $\epsilon$ -regime.

Let us again end by commenting on the conventional limit of large volumes. Assuming  $x_0 = -|x_0|$ ,  $y_0 = |y_0|$ , and inserting the unquenched value of  $E(x; M^2)$ , we obtain for the normalised case

$$\begin{aligned} [C_8']_{\text{norm}}^{ab}(x_0, y_0) = & -\{T^a, T^b\}_{ds} \left\{ 1 + \frac{M^2}{(4\pi F)^2} \left[ -N_f \left( 1 + \ln \frac{\Lambda^2}{M^2} \right) - \frac{2}{N_f} \ln \frac{\Lambda^2}{M^2} - \right. \right. \\ & \left. \left. - \frac{N_f}{2} \left\{ e^{-2M|x_0|} \Delta(2M|x_0|) + e^{-2M|y_0|} \Delta(2M|y_0|) \right\} + \right. \right. \end{aligned}$$



Figure 7: The leading-order graphs for  $[\mathcal{C}'_8]^{ab}(x_0, y_0)$  in the  $\epsilon$ -regime. An open square denotes the left-handed current, an open circle the weak operator, and a filled circle a mass insertion.

$$+ \frac{2}{N_f} \left\{ e^{-2M|x_0|} \Upsilon(2M|x_0|) + e^{-2M|y_0|} \Upsilon(2M|y_0|) \right\} \right\}, \quad (5.17)$$

where

$$\Delta(x) \equiv \int_0^\infty dz z^{\frac{1}{2}} e^{-xz} \frac{\sqrt{2+z}}{1+z} \left[ \frac{2}{2+z} \right], \quad (5.18)$$

$$\Upsilon(x) \equiv \int_0^\infty dz z^{\frac{1}{2}} e^{-xz} \frac{\sqrt{2+z}}{1+z} \left[ \frac{1}{2+z} + \frac{1}{1+z} \right]. \quad (5.19)$$

This result is plotted in Fig. 6(right) with dotted lines. We observe again how only values  $ML \gtrsim 5.0$  guarantee that finite-volume effects are small ( $\lesssim 20\%$ ).

## 5.2. $\epsilon$ -regime

We finally move to the  $\epsilon$ -regime. For  $\mathcal{C}_8$  the graphs are the same as for  $\mathcal{C}_{27}$ , as depicted in Fig. 3 of Ref. [19]. The correlator retains the form in Eq. (5.2), with  $\Delta_8^{ab}$  from Eq. (5.3),  $\mathcal{C}(x_0)$  from Eq. (3.10), and  $\mathcal{D}_{27}(x_0, y_0)$ , appearing as in Eq. (5.5), from Eq. (4.12). The order of magnitude of the leading term in  $[\mathcal{C}_8]^{ab}(x_0, y_0)$  is  $O(\epsilon^2)$ , and the NLO term is  $O(\epsilon^4)$ , while the terms beyond  $\mathcal{D}_{27}(x_0, y_0)$  in Eq. (5.5) are formally  $O(\epsilon^6)$ , so that the corresponding graph (the sixth in Fig. 2) can be ignored in the  $\epsilon$ -regime. Therefore, all information is in the  $\epsilon$ -regime version of  $\mathcal{D}_{27}(x_0, y_0)$ . To be explicit, the normalised form of Eq. (5.10) becomes

$$[\mathcal{C}_8]_{\text{norm}}^{ab}(x_0, y_0) = \Delta_8^{ab} \left[ 1 - \frac{N_v}{(FL)^2} \left( \rho^{-\frac{1}{2}} \beta_1 - \rho k_{00} \right) \right]. \quad (5.20)$$

Let us stress, in particular, that  $[\mathcal{C}_8]_{\text{norm}}^{ab}(x_0, y_0)$  is independent of topology and quenching at this order, just like  $[\mathcal{C}_{27}]_{\text{norm}}^{ab}(x_0, y_0)$ . (However, as discussed at the end of Appendix C, quenching does lead to the appearance of additional LECs [32] that need to be disentangled.)

Let us then address  $\mathcal{C}'_8$ . Given that the  $\epsilon$ -regime computation is to be carried out at fixed topology, the operator  $\mathcal{O}'_8$  needs now to be considered in the full generality of Eq. (2.14), i.e., with a non-vanishing vacuum angle  $\theta$ , unlike in the  $p$ -regime. Therefore  $\mathcal{O}'_8$  can also couple to an odd number of Goldstone fields. On the other hand, it is easy to see that the tree-level graphs (cf. Fig. 7) are already of order  $O(\epsilon^4)$ . Comparing with  $\mathcal{C}_8$ , it is therefore enough to

restrict to the leading order. We find

$$\begin{aligned} [\mathcal{C}'_8]^{ab}(x_0, y_0) &= \frac{\mu F^2}{2V} \left\{ \{T^a \cdot T^b\}_{ds} \left[ \sigma_\nu(\mu) h'_1(\hat{x}_0) h'_1(\hat{y}_0) + \right. \right. \\ &\quad + \frac{\mu}{1 - N_f^2} \left\{ \sigma'_\nu(\mu) + N_f \sigma_\nu^2(\mu) + N_f^2 \frac{\sigma_\nu(\mu)}{\mu} - N_f \left( 1 + \frac{\nu^2}{\mu^2} \right) \right\} h_1(\hat{x}_0 - \hat{y}_0) \Big] + \\ &\quad \left. \left. + [T^a, T^b]_{ds} \frac{\nu}{\mu} \left\{ h'_1(\hat{x}_0 - \hat{y}_0) [h'_1(\hat{x}_0) + h'_1(\hat{y}_0)] + h_1(\hat{y}_0) - h_1(\hat{x}_0) \right\} \right\}, \quad (5.21) \right. \end{aligned}$$

where  $h_1$  is from Eq. (3.16). The corresponding normalised form reads

$$[\mathcal{C}'_8]_{\text{norm}}^{ab}(x_0, y_0) = \frac{4T^2}{F^4} [\mathcal{C}'_8]^{ab}(x_0, y_0). \quad (5.22)$$

This result is to be used in combination with Eq. (5.20), in order to disentangle the two terms on the right-hand side of Eq. (5.1).

Unlike Eq. (5.20), the expressions in Eqs. (5.21), (5.22) get modified in the quenched theory, because they contain Goldstone zero-mode integrals. Proceeding as in Ref. [16], we find

$$\begin{aligned} [\mathcal{C}'_8]_q^{ab}(x_0, y_0) &= \frac{\mu F^2}{2V} \left\{ \{T^a \cdot T^b\}_{ds} \left[ \sigma_{q\nu}(\mu) h'_1(\hat{x}_0) h'_1(\hat{y}_0) + \mu \sigma'_{q\nu}(\mu) h_1(\hat{x}_0 - \hat{y}_0) \right] + \right. \\ &\quad \left. + [T^a, T^b]_{ds} \frac{\nu}{\mu} \left\{ h'_1(\hat{x}_0 - \hat{y}_0) [h'_1(\hat{x}_0) + h'_1(\hat{y}_0)] + h_1(\hat{y}_0) - h_1(\hat{x}_0) \right\} \right\}, \quad (5.23) \end{aligned}$$

where the subscript  $q$  refers to the quenched theory, and [57]

$$\sigma_{q\nu}(\mu) \equiv \mu \left[ I_\nu(\mu) K_\nu(\mu) + I_{\nu+1}(\mu) K_{\nu-1}(\mu) \right] + \frac{\nu}{\mu}, \quad (5.24)$$

where  $I_\nu, K_\nu$  are modified Bessel functions. Note that Eq. (5.23) could also be obtained from Eq. (5.21) by just naively setting  $N_f \rightarrow 0$  and replacing  $\sigma_\nu \rightarrow \sigma_{q\nu}$ .

Since the functions  $[\mathcal{C}_8]^{ab}(x_0, y_0)$  and  $[\mathcal{C}'_8]^{ab}(x_0, y_0)$  are not identical, a precise measurement of the time-dependence of the correlation function of the left-hand side of Eq. (5.1) would in principle allow to disentangle the contributions to  $g_8, g'_8$ . In particular, as shown in Fig. 5, any dependence of the correlation functions on  $\nu$  arises at this order through the operator  $\mathcal{O}'_8$ . In practice, however, the problem emerges that it may not be easy to obtain such a high accuracy that the two LECs could reliably be determined from a single observable. Therefore, it may be beneficial to define another probe as well, such that the LECs can be disentangled with better confidence. We now show how this can be done.

### 5.3. Direct determination of $g'_8$

In order to determine  $g'_8$ , we consider the correlator

$$[K_R]^a(x_0) \equiv \int d^3x \left\langle J_0^a(x) O_R(0) \right\rangle, \quad (5.25)$$

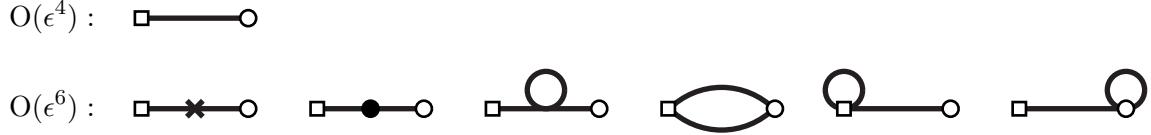


Figure 8: The graphs contributing to  $[\mathcal{K}'_8]^a(x_0)$ . The notation is as in Fig. 7, with additionally a cross denoting a ‘measure term’ (cf. Ref. [9]).

on the side of QCD, and correspondingly

$$[\mathcal{K}_R]^a(x_0) \equiv \int d^3x \left\langle \mathcal{J}_0^a(x) \mathcal{O}_R(0) \right\rangle \quad (5.26)$$

on the  $\chi$ PT side. Note that this correlation function is not available in the conventional  $p$ -regime setup (i.e. with  $\theta = 0$ ), because it is odd in charge conjugation.

We have computed both  $[\mathcal{K}_8]^a(x_0)$  and  $[\mathcal{K}'_8]^a(x_0)$  at NLO in the  $\epsilon$ -regime. Parametrically, the orders of magnitude of the LO and the NLO graphs are  $O(\epsilon^4)$  and  $O(\epsilon^6)$ , respectively. We find, however, that at this order  $[\mathcal{K}_8]^a(x_0)$  vanishes exactly, like in the  $p$ -regime.

On the other hand,  $[\mathcal{K}'_8]^a(x_0)$  does not vanish. The graphs are shown in Fig. 8. We find

$$[\mathcal{K}'_8]^a(x_0) = -T_{ds}^a \frac{\nu F^2}{V} \left\{ h'_1(\hat{x}_0) \left[ 1 + \left( \frac{1}{N_f} - N_f \right) \frac{\bar{G}(0)}{F^2} \right] + h'_2(\hat{x}_0) \frac{2T^2}{F^2 V} \left[ \mu \sigma_\nu(\mu) + \frac{1}{N_f} \right] \right\}, \quad (5.27)$$

where  $\bar{G}(x)$  is from Eq. (3.11), and (for  $|\tau| \leq 1$ )

$$h_2(\tau) \equiv \frac{1}{24} \left[ \tau^2 (|\tau| - 1)^2 - \frac{1}{30} \right]. \quad (5.28)$$

The result is illustrated in Fig. 9, after normalisation through

$$\frac{L^3 [\mathcal{K}'_8]^a(x_0)}{\mathcal{C}(x_0)} \equiv T_{ds}^a [\mathcal{K}'_8]_{\text{norm}}(x_0). \quad (5.29)$$

Repeating the same steps in the quenched theory, we find

$$\begin{aligned} [\mathcal{K}'_8]^a_{\text{q}}(x_0) &= -T_{ds}^a \frac{\nu F^2}{V} \left\{ h'_1(\hat{x}_0) \left[ 1 + \frac{\alpha}{2N_c} \frac{\bar{G}(0)}{F^2} + \frac{m_0^2}{2N_c} \frac{\bar{H}(0)}{F^2} \right] + \right. \\ &\quad \left. + \frac{2T^2}{F^2 V} \left[ \left( \mu \sigma_{q\nu}(\mu) + \frac{\alpha}{2N_c} \right) h'_2(\hat{x}_0) - \frac{m_0^2 T^2}{2N_c} h'_3(\hat{x}_0) \right] \right\}, \end{aligned} \quad (5.30)$$

where  $\bar{H}(x)$  and  $h_3(\tau)$  (for  $|\tau| \leq 1$ ) are defined through

$$\bar{H}(x) \equiv \frac{1}{V} \sum_{n \in \mathbb{Z}^4} \left( 1 - \delta_{n,0}^{(4)} \right) \frac{e^{ip \cdot x}}{(p^2)^2}, \quad (5.31)$$

$$h_3(\tau) \equiv \frac{1}{720} \left[ \tau^2 (|\tau| - 1)^2 \left( \tau^2 - |\tau| - \frac{1}{2} \right) + \frac{1}{42} \right]. \quad (5.32)$$

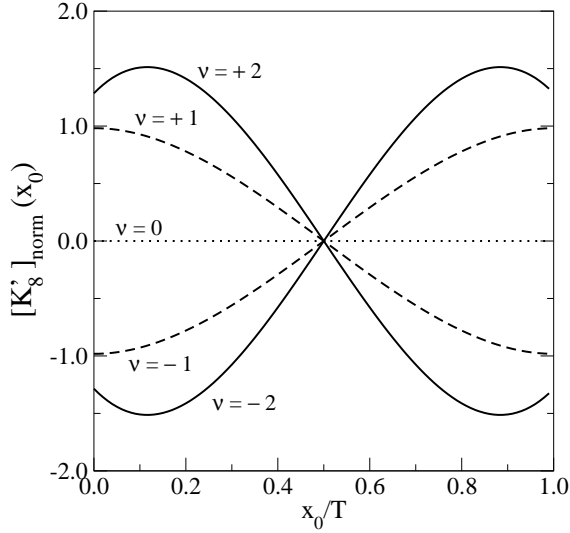


Figure 9: The function  $[K'_8]_{\text{norm}}(x_0)$  as a function of  $x_0$  and  $\nu$ . The other parameters are:  $N_f = 3$ ,  $F = 93$  MeV,  $\mu = 2.0$ ,  $L = 2$  fm,  $T/L = 2$ .

The value of  $\bar{H}(0)$  is given by [47]

$$\bar{H}(0) = \beta_2 + \frac{\mu^{-2\epsilon}}{(4\pi)^2} \left[ \frac{1}{\epsilon} + \ln(\bar{\mu}^2 V^{1/2}) + 1 + O(\epsilon) \right], \quad (5.33)$$

where  $\ln \bar{\mu}^2 \equiv \ln \mu^2 + \ln 4\pi - \gamma_E$ , and (with  $\hat{\alpha}$  from Eq. (3.13))

$$\beta_2 = \frac{1}{(4\pi)^2} \left[ \hat{\alpha}_0 \left( \rho^{\frac{3}{4}}, \rho^{-\frac{1}{4}} \right) + \hat{\alpha}_{-2} \left( \rho^{-\frac{3}{4}}, \rho^{\frac{1}{4}} \right) - \frac{3}{2} - \ln(4\pi) + \gamma_E \right]. \quad (5.34)$$

The UV-divergence in Eq. (5.33) is cancelled by  $\Sigma$  (cf. Eq. (2.14)), which is to be treated as a bare parameter in the quenched theory [58].

To summarise, we now have a method to disentangle the two contributions related to the LECs  $g_8, g'_8$ : by considering  $[K'_8]_{\text{norm}}(x_0)$ , we can first match for  $g'_8$ . Then the corresponding term can be subtracted from the right-hand side of Eq. (5.1), and we are able to determine  $g_8$ . As illustrated in Fig. 5, a cross-check is that the dependence on  $\nu$  should have disappeared.

#### 5.4. Further remarks

The remarks that can be made on the convergence of the  $\epsilon$  and  $p$ -regime computations of  $\mathcal{C}_8$  and  $\mathcal{C}'_8$  are largely the same as for  $\mathcal{C}_{27}$  in Sec. 4.3. Indeed, for  $1/FL \ll 1$ , there could be a non-vanishing overlap, i.e. a regime where both the  $p$ -regime and the  $\epsilon$ -regime expressions are valid. For the more realistic case  $1/FL \sim 1$ , on the other hand, this is unlikely to happen. It would be tempting to read from Fig. 6 that the  $p$ -regime expression works in the range  $ML \gtrsim 2.0$ , and the  $\epsilon$ -regime expression in the range  $\mu \lesssim 2.0$ , but whether this is really the case remains to be seen once a comparison with lattice simulation results is available.

Concerning quenching, let us stress that the correlation function  $[\mathcal{C}_8]_{\text{norm}}^{ab}(x_0, y_0)$  is determined in the  $\epsilon$ -regime by the same function  $\mathcal{R}_{27}(x_0, y_0)$  as  $[\mathcal{C}_{27}]_{\text{norm}}^{ab}(x_0, y_0)$ , and is thus insensitive to quenching at the present order. At the same time, the correlation functions  $[\mathcal{C}'_8]_{\text{norm}}^{ab}(x_0, y_0)$  and  $[\mathcal{K}'_8]_{\text{norm}}^a(x_0)$  do get modified.

An important point however is the different relevance of the quenched ambiguities of Ref. [32] in the two regimes. In general the quenched theory contains spurious operators with new LECs. Some of these originate from the fact that  $N_f \neq N_v$ , a case that is considered in detail in Appendix C, while others are related to the couplings of the axial singlet field that cannot be integrated out in the quenched limit. The latter modify the terms that in the full theory would be divergent in the limit  $N_f \rightarrow 0$ . We indeed confirm a rather messy situation in the  $p$ -regime, where many new couplings enter; thus we have not carried out a systematic study of all quenching effects in our observables in this regime. On the other hand, the quenching ambiguities are reduced to a minimum at the NLO in the  $\epsilon$ -regime, with apparently only one spurious octet LEC contributing to the “physical part”  $[\mathcal{C}_8]_{\text{norm}}^{ab}(x_0, y_0)$ . Therefore a certain combination of octet couplings *can* be determined by matching the lattice simulation results to  $[\mathcal{C}_8]_{\text{norm}}^{ab}(x_0, y_0)$ . We elaborate on this issue in more detail in Appendix C, particularly around Eq. (C.23).

## 6. Conclusions

We have addressed in this paper the determination of the  $\mathcal{O}(p^2)$  LECs of the chiral weak Hamiltonian. As probes we have used the three-point correlation functions between the weak operators and left-handed flavour currents. We have computed the three-point correlation functions up to next-to-leading order in chiral perturbation theory, both in the  $\epsilon$  and in the  $p$ -regimes, for all three operators that appear in the SU(3) chiral weak Hamiltonian.

While the determination of the LEC  $g_{27}$ , which fixes the  $\Delta I = 3/2$  amplitude of the weak decays  $K \rightarrow \pi\pi$  as well as the kaon mixing parameter  $\hat{B}_K$  in the chiral limit, appears straightforward, the determination of the LECs fixing the  $\Delta I = 1/2$  amplitudes is more demanding in several respects. Even restricting to the idealised case of full QCD at large volumes, there are two operators with the same flavour symmetry, while only the coefficient of one of them,  $g_8$ , contributes to the physical kaon decays [3, 4]. Therefore it is important to come up with a setup which allows to remove the contamination from the other operator in a lattice measurement of the type that we have considered.

We have shown here that this challenge can be met in a straightforward way by going to the  $\epsilon$ -regime. The two operators contribute in very different ways to a given three-point correlation function, one leading to a topology-dependent and the other to a topology-independent result. Moreover, we have found a two-point correlator which allows to determine the “unphysical” LEC directly. Therefore, it seems possible in principle to disentangle the physical coefficient  $g_8$  from lattice measurements in the  $\epsilon$ -regime.

By comparing the  $\epsilon$ -regime results with  $p$ -regime results in a finite volume, we have also speculated on the regimes of validity of the two approaches. It appears that for semi-realistic lattices with a spatial extent of about 2 fm, the  $\epsilon$ -regime approach might be applicable for  $\mu = m\Sigma V \lesssim 2.0$  and the  $p$ -regime for  $ML \gtrsim 2.0$ . In any case, the conventional infinite-volume formulae are accurate (with errors below 10 – 20%) only at  $ML \gtrsim 5.0$ .

Finally, we have briefly addressed the effect of quenching on the determination of the  $\Delta I = 1/2$  observables. It appears that in the  $\epsilon$ -regime unphysical contributions can practically be eliminated at NLO such that even quenched simulations may be used for first numerical measurements of the correlation functions that we have computed in this paper.

## Acknowledgements

This work is part of a bigger effort whose goal is to extract low-energy constants of QCD from numerical simulations with Ginsparg-Wilson fermions. We are indebted to our collaborators on this, L. Giusti, C. Pena, J. Wennekers and H. Wittig, for useful comments. The basic ideas of the general approach were developed in collaboration with M. Lüscher and P. Weisz; we would like to thank them for their input and for many valuable suggestions. P. H. was supported in part by the Spanish CICYT (Project No. FPA2004-00996 and FPA2005-01678) and by the Generalitat Valenciana (Project No. GVA05/164).

## Appendix A. Irreducible representations of the valence group

For completeness, we reiterate in this Appendix the main formulae related to irreducible representations of the valence group  $SU(N_v)$ , relevant for the operators appearing in the weak Hamiltonian. We follow the tensor method discussed, e.g., in Ref. [59].

Like in the main body of the text, we make a distinction between the valence group  $SU(N_v)$ , used to classify the weak operators, and the full flavour symmetry  $SU(N_f)$ . The indices  $\bar{r}, \bar{s}, \bar{u}, \bar{v}, \tilde{r}, \tilde{s}, \tilde{u}, \tilde{v}, \hat{r}, \hat{s}, \hat{u}, \hat{v}$  are assumed to take values in the valence subgroup only. We denote by  $O_{\bar{r}\bar{s}\bar{u}\bar{v}}$  a generic operator transforming under  $\mathbf{N}_v^* \otimes \mathbf{N}_v^* \otimes \mathbf{N}_v \otimes \mathbf{N}_v$  of  $SU(N_v)$ , and by  $O'_{\tilde{r}\tilde{u}}$  one transforming under  $\mathbf{N}_v^* \otimes \mathbf{N}_v$ .

We define the projection operators

$$(P_1^\sigma)_{\bar{r}\bar{s}\bar{u}\bar{v};\tilde{r}\tilde{s}\tilde{u}\tilde{v}} \equiv \frac{1}{4}(\delta_{\bar{r}\tilde{r}}\delta_{\bar{s}\tilde{s}} + \sigma\delta_{\bar{r}\tilde{s}}\delta_{\bar{s}\tilde{r}})(\delta_{\bar{u}\tilde{u}}\delta_{\bar{v}\tilde{v}} + \sigma\delta_{\bar{u}\tilde{v}}\delta_{\bar{v}\tilde{u}}) , \quad (\text{A.1})$$

$$(P_2^\sigma)_{\bar{r}\bar{s}\bar{u}\bar{v};\tilde{r}\tilde{s}\tilde{u}\tilde{v}} \equiv \delta_{\bar{r}\tilde{r}}\delta_{\bar{s}\tilde{s}}\delta_{\bar{u}\tilde{u}}\delta_{\bar{v}\tilde{v}} + \frac{1}{(N_v + 2\sigma)(N_v + \sigma)}(\delta_{\bar{r}\bar{u}}\delta_{\bar{s}\bar{v}} + \sigma\delta_{\bar{r}\bar{v}}\delta_{\bar{s}\bar{u}})\delta_{\tilde{r}\tilde{u}}\delta_{\tilde{s}\tilde{v}} - \frac{1}{N_v + 2\sigma}(\delta_{\bar{r}\bar{u}}\delta_{\bar{s}\tilde{s}}\delta_{\bar{v}\tilde{v}}\delta_{\tilde{r}\tilde{u}} + \delta_{\bar{s}\bar{v}}\delta_{\bar{r}\tilde{r}}\delta_{\bar{u}\tilde{u}}\delta_{\tilde{s}\tilde{v}} + \sigma\delta_{\bar{r}\bar{v}}\delta_{\bar{s}\tilde{s}}\delta_{\bar{u}\tilde{v}}\delta_{\tilde{r}\tilde{u}} + \sigma\delta_{\bar{s}\bar{u}}\delta_{\bar{r}\tilde{r}}\delta_{\bar{v}\tilde{u}}\delta_{\tilde{s}\tilde{v}}) , \quad (\text{A.2})$$

$$(P_3)_{\bar{r}\bar{u};\tilde{r}\tilde{u}} \equiv \delta_{\bar{r}\tilde{r}}\delta_{\bar{u}\tilde{u}} - \frac{1}{N_v}\delta_{\bar{r}\bar{u}}\delta_{\tilde{r}\tilde{u}} . \quad (\text{A.3})$$

In addition,  $P_v$  is defined to project from  $SU(N_f)$  to  $SU(N_v)$ . The operators denoted by  $O_{27}$ ,  $O_8$  and  $O'_8$  can now be defined as

$$[O_{27}]_{\bar{r}\bar{s}\bar{u}\bar{v}} \equiv (P_2^+ P_1^+)_{\bar{r}\bar{s}\bar{u}\bar{v};\tilde{r}\tilde{s}\tilde{u}\tilde{v}} O_{\tilde{r}\tilde{s}\tilde{u}\tilde{v}} , \quad (\text{A.4})$$

$$[O_8^\pm]_{\bar{r}\bar{u}} \equiv (P_3)_{\bar{r}\bar{u};\tilde{r}\tilde{u}} (P_1^\pm)_{\tilde{r}\tilde{s}\tilde{u}\tilde{s};\bar{r}\bar{s}\bar{u}\bar{v}} O_{\bar{r}\bar{s}\bar{u}\bar{v}} , \quad (\text{A.5})$$

$$[O'_8]_{\bar{r}\bar{u}} \equiv (P_3)_{\bar{r}\bar{u};\tilde{r}\tilde{u}} O'_{\tilde{r}\tilde{u}} . \quad (\text{A.6})$$

Note that the contraction over  $\hat{s}$  in Eq. (A.5) goes over valence flavours only, and that additional octet operators ( $O_8^-$ ) can appear already at the leading order when  $N_v \neq N_f$ .

Instead of a generic operator  $O_{\bar{r}\bar{s}\bar{u}\bar{v}}$ , practical computations of the type in Ref. [60] involve certain factorised forms, like

$$[O_1]_{\bar{r}\bar{s}\bar{u}\bar{v}} \equiv (Q)_{\bar{u}\bar{r}}(R)_{\bar{v}\bar{s}} , \quad (\text{A.7})$$

$$[O_2]_{\bar{r}\bar{s}\bar{u}\bar{v}} \equiv (Q)_{\bar{u}\bar{s}}(R)_{\bar{v}\bar{r}} , \quad (\text{A.8})$$

$$[O_3]_{\bar{r}\bar{s}\bar{u}\bar{v}} \equiv \delta_{\bar{u}\bar{r}}(R)_{\bar{v}\bar{s}} , \quad (\text{A.9})$$

$$[O_4]_{\bar{r}\bar{s}\bar{u}\bar{v}} \equiv \delta_{\bar{u}\bar{s}}(R)_{\bar{v}\bar{r}} , \quad (\text{A.10})$$

$$[O_5]_{\bar{r}\bar{s}\bar{u}\bar{v}} \equiv \delta_{\bar{u}\bar{r}}\delta_{\bar{v}\bar{s}} , \quad (\text{A.11})$$

$$[O_6]_{\bar{r}\bar{s}\bar{u}\bar{v}} \equiv \delta_{\bar{u}\bar{s}}\delta_{\bar{v}\bar{r}} . \quad (\text{A.12})$$

Then projections of the types in Eqs. (A.4), (A.5) produce

$$\begin{aligned}
[P_2^\sigma P_1^\sigma O_1]_{\bar{r}\bar{s}\bar{u}\bar{v}} &= S_{\bar{r}\bar{s}\bar{u}\bar{v}}^\sigma(Q, R), & [P_3 P_1^\sigma O_1]_{\bar{r}\bar{u}} &= T_{\bar{r}\bar{u}}^\sigma(Q, R), \\
[P_2^\sigma P_1^\sigma O_2]_{\bar{r}\bar{s}\bar{u}\bar{v}} &= \sigma S_{\bar{r}\bar{s}\bar{u}\bar{v}}^\sigma(Q, R), & [P_3 P_1^\sigma O_2]_{\bar{r}\bar{u}} &= \sigma T_{\bar{r}\bar{u}}^\sigma(Q, R), \\
[P_2^\sigma P_1^\sigma O_3]_{\bar{r}\bar{s}\bar{u}\bar{v}} &= 0, & [P_3 P_1^\sigma O_3]_{\bar{r}\bar{u}} &= U_{\bar{r}\bar{u}}^\sigma(R), \\
[P_2^\sigma P_1^\sigma O_4]_{\bar{r}\bar{s}\bar{u}\bar{v}} &= 0, & [P_3 P_1^\sigma O_4]_{\bar{r}\bar{u}} &= \sigma U_{\bar{r}\bar{u}}^\sigma(R), \\
[P_2^\sigma P_1^\sigma O_5]_{\bar{r}\bar{s}\bar{u}\bar{v}} &= 0, & [P_3 P_1^\sigma O_5]_{\bar{r}\bar{u}} &= 0, \\
[P_2^\sigma P_1^\sigma O_6]_{\bar{r}\bar{s}\bar{u}\bar{v}} &= 0, & [P_3 P_1^\sigma O_6]_{\bar{r}\bar{u}} &= 0,
\end{aligned} \tag{A.13}$$

where (introducing the notation  $\text{Tr}_v(\dots) \equiv \text{Tr}(P_v \dots)$ )

$$\begin{aligned}
S_{\bar{r}\bar{s}\bar{u}\bar{v}}^\sigma(Q, R) &= \frac{1}{4} \left\{ Q_{\bar{u}\bar{r}} R_{\bar{v}\bar{s}} + R_{\bar{u}\bar{r}} Q_{\bar{v}\bar{s}} + \sigma(Q_{\bar{u}\bar{s}} R_{\bar{v}\bar{r}} + R_{\bar{u}\bar{s}} Q_{\bar{v}\bar{r}}) - \right. \\
&\quad - \frac{\delta_{\bar{v}\bar{r}}}{N_v + 2\sigma} \left[ (QP_v R + RP_v Q)_{\bar{u}\bar{s}} + \sigma(Q_{\bar{u}\bar{s}} \text{Tr}_v(R) + R_{\bar{u}\bar{s}} \text{Tr}_v(Q)) \right] - \\
&\quad - \frac{\delta_{\bar{u}\bar{s}}}{N_v + 2\sigma} \left[ (QP_v R + RP_v Q)_{\bar{v}\bar{r}} + \sigma(Q_{\bar{v}\bar{r}} \text{Tr}_v(R) + R_{\bar{v}\bar{r}} \text{Tr}_v(Q)) \right] - \\
&\quad - \frac{\sigma \delta_{\bar{u}\bar{r}}}{N_v + 2\sigma} \left[ (QP_v R + RP_v Q)_{\bar{v}\bar{s}} + \sigma(Q_{\bar{v}\bar{s}} \text{Tr}_v(R) + R_{\bar{v}\bar{s}} \text{Tr}_v(Q)) \right] - \\
&\quad - \frac{\sigma \delta_{\bar{v}\bar{s}}}{N_v + 2\sigma} \left[ (QP_v R + RP_v Q)_{\bar{u}\bar{r}} + \sigma(Q_{\bar{u}\bar{r}} \text{Tr}_v(R) + R_{\bar{u}\bar{r}} \text{Tr}_v(Q)) \right] + \\
&\quad \left. + \frac{2(\delta_{\bar{u}\bar{s}} \delta_{\bar{v}\bar{r}} + \delta_{\bar{u}\bar{r}} \delta_{\bar{v}\bar{s}})}{(N_v + \sigma)(N_v + 2\sigma)} \left[ \text{Tr}_v(QP_v R) + \sigma \text{Tr}_v(Q) \text{Tr}_v(R) \right] \right\}, \tag{A.14}
\end{aligned}$$

$$\begin{aligned}
T_{\bar{r}\bar{u}}^\sigma(Q, R) &= \frac{1}{4} \left[ \sigma(QP_v R + RP_v Q)_{\bar{u}\bar{r}} + Q_{\bar{u}\bar{r}} \text{Tr}_v(R) + R_{\bar{u}\bar{r}} \text{Tr}_v(Q) \right] - \\
&\quad - \frac{\delta_{\bar{u}\bar{r}}}{2N_v} \left[ \text{Tr}_v(Q) \text{Tr}_v(R) + \sigma \text{Tr}_v(QP_v R) \right], \tag{A.15}
\end{aligned}$$

$$U_{\bar{r}\bar{u}}^\sigma(R) = \frac{1}{4}(N_v + 2\sigma) \left[ R_{\bar{u}\bar{r}} - \frac{\delta_{\bar{u}\bar{r}}}{N_v} \text{Tr}_v(R) \right]. \tag{A.16}$$

Considering, in particular, the operators

$$\Delta_{\bar{r}\bar{s}\bar{u}\bar{v}}^{(1)} = T_{\bar{u}\bar{r}}^{\{a} T_{\bar{v}\bar{s}}^{b\}}, \tag{A.17}$$

$$\Delta_{\bar{r}\bar{s}\bar{u}\bar{v}}^{(2)} = T_{\bar{u}\bar{s}}^{\{a} T_{\bar{v}\bar{r}}^{b\}} - \frac{1}{2} \left( \delta_{\bar{u}\bar{s}} \{T^a, T^b\}_{\bar{v}\bar{r}} + \delta_{\bar{v}\bar{r}} \{T^a, T^b\}_{\bar{u}\bar{s}} \right), \tag{A.18}$$

$$\Delta_{\bar{r}\bar{s}\bar{u}\bar{v}}^{(3)} = T_{\bar{u}\bar{s}}^{\{a} T_{\bar{v}\bar{r}}^{b\}} + \delta_{\bar{u}\bar{s}} \{T^a, T^b\}_{\bar{v}\bar{r}} + \delta_{\bar{v}\bar{r}} \{T^a, T^b\}_{\bar{u}\bar{s}}, \tag{A.19}$$

$$\Delta_{\bar{r}\bar{s}\bar{u}\bar{v}}^{(4)} = \delta_{\bar{u}\bar{r}} \{T^a, T^b\}_{\bar{v}\bar{s}} + \delta_{\bar{v}\bar{s}} \{T^a, T^b\}_{\bar{u}\bar{r}}, \tag{A.20}$$

which appear in the computations of Fig. 2, and choosing the indices that appear in the

physical operators  $O_{27}$  and  $O_8$ , we obtain

$$\begin{aligned}
[P_2^+ P_1^+ \Delta^{(1)}]_{suud} &= 2S_{suud}^+(T^a, T^b), & [P_3 P_1^\sigma \Delta^{(1)}]_{sd} &= \frac{1}{2}\{T^a, T^b\}_{ds} \sigma, \\
[P_2^+ P_1^+ \Delta^{(2)}]_{suud} &= 2S_{suud}^+(T^a, T^b), & [P_3 P_1^\sigma \Delta^{(2)}]_{sd} &= \frac{1}{2}\{T^a, T^b\}_{ds} \left(-\frac{\sigma}{2} N_v\right), \\
[P_2^+ P_1^+ \Delta^{(3)}]_{suud} &= 2S_{suud}^+(T^a, T^b), & [P_3 P_1^\sigma \Delta^{(3)}]_{sd} &= \frac{1}{2}\{T^a, T^b\}_{ds} (\sigma N_v + 3), \\
[P_2^+ P_1^+ \Delta^{(4)}]_{suud} &= 0, & [P_3 P_1^\sigma \Delta^{(4)}]_{sd} &= \frac{1}{2}\{T^a, T^b\}_{ds} (N_v + 2\sigma).
\end{aligned} \tag{A.21}$$

For  $N_v = 3$ , the function  $\Delta_{27}^{ab} \equiv 2S_{suud}^+(T^a, T^b)$  is shown explicitly in Eq. (4.2).

## Appendix B. Ultraviolet divergences and $O(p^4)$ operators

Once we go beyond the order  $O(p^2)$  in  $\chi$ PT, the number of operators that enter Eq. (2.10) increases dramatically. At the order  $O(p^4)$ , we rewrite the weak Hamiltonian as

$$\mathcal{H}_w \equiv 2\sqrt{2}G_F V_{ud} V_{us}^* \left\{ \frac{5}{3} \left[ g_{27} \mathcal{O}_{27} + \sum_i D_i \bar{\mathcal{O}}_{27}^{(i)} \right] + 2 \left[ g_8 \mathcal{O}_8 + g'_8 \mathcal{O}'_8 + \sum_i E_i \bar{\mathcal{O}}_8^{(i)} \right] \right\} + \text{H.c.}, \tag{B.1}$$

where  $\bar{\mathcal{O}}_{27}^{(i)}$ ,  $\bar{\mathcal{O}}_8^{(i)}$  are the new operators. For  $N_f = N_v = 3$ , (over)complete sets for  $\bar{\mathcal{O}}_{27}^{(i)}$ ,  $\bar{\mathcal{O}}_8^{(i)}$  have been listed in Ref. [60]. The use of partial integration identities allows to reduce the number of operators drastically, leading to the lists commonly used in phenomenology [61]; in our case, however, the use of partial integration identities is not possible, since we consider local operator insertions (i.e.  $\mathcal{H}_w$  is not integrated over spacetime).

Generalizing Eq. (2.20), we define the correlation functions now with the LECs added,

$$[\mathcal{C}_{27}]^{ab}(x_0, y_0) \equiv \int d^3x \int d^3y \left\langle \mathcal{J}_0^a(x) \left[ g_{27} \mathcal{O}_{27}(0) + \sum_i D_i \bar{\mathcal{O}}_{27}^{(i)}(0) \right] \mathcal{J}_0^b(y) \right\rangle, \tag{B.2}$$

$$[\mathcal{C}_8]^{ab}(x_0, y_0) \equiv \int d^3x \int d^3y \left\langle \mathcal{J}_0^a(x) \left[ g_8 \mathcal{O}_8(0) + g'_8 \mathcal{O}'_8(0) + \sum_i E_i \bar{\mathcal{O}}_8^{(i)}(0) \right] \mathcal{J}_0^b(y) \right\rangle. \tag{B.3}$$

The results can be written in the forms

$$[\mathcal{C}_{27}]^{ab}(x_0, y_0) = \Delta_{27}^{ab} \left\{ g_{27} \left[ \mathcal{C}(x_0) \mathcal{C}(y_0) + \mathcal{D}_{27}(x_0, y_0) \right] + \mathcal{E}_{27}(x_0, y_0) \right\}, \tag{B.4}$$

$$[\mathcal{C}_8]^{ab}(x_0, y_0) = \Delta_8^{ab} \left\{ g_8 \left[ \mathcal{C}(x_0) \mathcal{C}(y_0) + \mathcal{D}_8(x_0, y_0) \right] + g'_8 \mathcal{D}'_8(x_0, y_0) + \mathcal{E}_8(x_0, y_0) \right\}, \tag{B.5}$$

where  $\Delta_{27}^{ab} = 2S_{suud}^+(T^a, T^b)$  in the notation of Eq. (A.21), and  $\Delta_8^{ab} = \{T^a, T^b\}_{ds}/2$ .

The list of operators from Ref. [60] (modulo certain minus-signs) that can contribute to  $\mathcal{C}_{27}$  at NLO is constituted by the properly projected (cf. Appendix A) versions of:

$$\bar{\mathcal{O}}_{27}^{(2)} = -(\mathcal{P})_{\bar{u}\bar{r}}(\mathcal{P})_{\bar{v}\bar{s}}, \tag{B.6}$$

$$\bar{\mathcal{O}}_{27}^{(4)} = (\mathcal{L}_\mu)_{\bar{u}\bar{r}} \{ \mathcal{L}_\mu, \mathcal{S} \}_{\bar{v}\bar{s}}, \tag{B.7}$$

$$\bar{\mathcal{O}}_{27}^{(7)} = (\mathcal{L}_\mu)_{\bar{u}\bar{r}} (\mathcal{L}_\mu)_{\bar{v}\bar{s}} \text{Tr} (\mathcal{S}) , \quad (\text{B.8})$$

$$\bar{\mathcal{O}}_{27}^{(19)} = i (\mathcal{W}_{\mu\mu})_{\bar{u}\bar{r}} (\mathcal{P})_{\bar{v}\bar{s}} , \quad (\text{B.9})$$

$$\bar{\mathcal{O}}_{27}^{(20)} = - (\mathcal{L}_\mu)_{\bar{u}\bar{r}} (\partial_\nu \mathcal{W}_{\mu\nu})_{\bar{v}\bar{s}} , \quad (\text{B.10})$$

$$\bar{\mathcal{O}}_{27}^{(21)} = - (\mathcal{L}_\mu)_{\bar{u}\bar{r}} (\partial_\mu \mathcal{W}_{\nu\nu})_{\bar{v}\bar{s}} , \quad (\text{B.11})$$

$$\bar{\mathcal{O}}_{27}^{(24)} = - (\mathcal{W}_{\mu\nu})_{\bar{u}\bar{r}} (\mathcal{W}_{\mu\nu})_{\bar{v}\bar{s}} , \quad (\text{B.12})$$

$$\bar{\mathcal{O}}_{27}^{(25)} = - (\mathcal{W}_{\mu\mu})_{\bar{u}\bar{r}} (\mathcal{W}_{\nu\nu})_{\bar{v}\bar{s}} . \quad (\text{B.13})$$

Here we utilize the notation

$$\mathcal{S} \equiv U\chi^\dagger + \chi U^\dagger , \quad \mathcal{P} \equiv i \left( U\chi^\dagger - \chi U^\dagger \right) , \quad (\text{B.14})$$

$$\mathcal{L}_\mu \equiv U\partial_\mu U^\dagger , \quad \mathcal{W}_{\mu\nu} \equiv 2(\partial_\mu \mathcal{L}_\nu + \partial_\nu \mathcal{L}_\mu) , \quad (\text{B.15})$$

where  $\chi \equiv 2m\Sigma/F^2 = M^2$ . As stressed in Ref. [60], not all of these operators are independent, however: equations of motion can be used to eliminate 19, 21, and 25, for instance. In the following, we keep for generality all the operators.

The contribution from the  $\mathcal{O}(p^4)$ -constants to Eq. (B.4) reads

$$\begin{aligned} \mathcal{E}_{27}(x_0, y_0) &= 4M^4 P'(x_0) P'(y_0) [D_2 + 2D_{19} - 4D_{24} - 4D_{25}] + \\ &+ 4M^6 P(x_0) P(y_0) \left[ D_4 + \frac{N_f}{2} D_7 - D_{20} - D_{21} - F^2 (N_f L_4 + L_5) \right] . \end{aligned} \quad (\text{B.16})$$

Taking into account that  $\mathcal{C}(x_0)$  is finite; that  $\mathcal{D}_{27}(x_0, y_0)$  contains the divergences specified in Eq. (4.8); that the QCD  $\mathcal{O}(p^4)$  constants contain the divergence ( $\lambda \equiv -1/32\pi^2\epsilon$ )

$$N_f L_4 + L_5 = N_f L_4^r + L_5^r + \frac{N_f}{4} \lambda , \quad (\text{B.17})$$

where  $L_4^r$ ,  $L_5^r$  are finite; and that the  $\mathcal{O}(p^4)$  constants contain the divergences

$$\begin{aligned} D_4 &= D_4^r + g_{27} F^2 \lambda \left( \frac{N_f + 3}{8} \right) , \\ D_7 &= D_7^r + g_{27} F^2 \lambda \left( \frac{1}{4} \right) , \\ D_{20} &= D_{20}^r + g_{27} F^2 \lambda \left( \frac{1}{8} \right) , \\ D_{24} &= D_{24}^r + g_{27} F^2 \lambda \left( \frac{1}{32} \right) , \end{aligned} \quad (\text{B.18})$$

the correlation function  $\mathcal{C}_{27}$  in Eq. (B.4) can be seen to be finite.

As far as the octet correlation functions are concerned, it is the following types among the operators listed in Ref. [60] that contribute to the correlation function  $\mathcal{C}_8$  at the order we are considering:

$$\bar{\mathcal{O}}_8^{(1)} \equiv -(\mathcal{S}\mathcal{S})_{ds} , \quad (\text{B.19})$$

$$\bar{\mathcal{O}}_8^{(2)} \equiv -(\mathcal{S})_{ds} \text{Tr}(\mathcal{S}) , \quad (\text{B.20})$$

$$\bar{\mathcal{O}}_8^{(3)} \equiv -(\mathcal{P}\mathcal{P})_{ds} , \quad (\text{B.21})$$

$$\bar{\mathcal{O}}_8^{(10)} \equiv \{\mathcal{S}, \mathcal{L}_\mu \mathcal{L}_\mu\}_{ds} , \quad (\text{B.22})$$

$$\bar{\mathcal{O}}_8^{(11)} \equiv (\mathcal{L}_\mu \mathcal{S} \mathcal{L}_\mu)_{ds} , \quad (\text{B.23})$$

$$\bar{\mathcal{O}}_8^{(14)} \equiv (\mathcal{L}_\mu \mathcal{L}_\mu)_{ds} \text{Tr}(\mathcal{S}) , \quad (\text{B.24})$$

$$\bar{\mathcal{O}}_8^{(33)} \equiv i\{\mathcal{W}_{\mu\mu}, \mathcal{P}\}_{ds} , \quad (\text{B.25})$$

$$\bar{\mathcal{O}}_8^{(35)} \equiv -\{\mathcal{L}_\mu, \partial_\nu \mathcal{W}_{\mu\nu}\}_{ds} , \quad (\text{B.26})$$

$$\bar{\mathcal{O}}_8^{(36)} \equiv -\{\mathcal{L}_\mu, \partial_\mu \mathcal{W}_{\nu\nu}\}_{ds} , \quad (\text{B.27})$$

$$\bar{\mathcal{O}}_8^{(39)} \equiv -(\mathcal{W}_{\mu\nu} \mathcal{W}_{\mu\nu})_{ds} , \quad (\text{B.28})$$

$$\bar{\mathcal{O}}_8^{(40)} \equiv -(\mathcal{W}_{\mu\mu} \mathcal{W}_{\nu\nu})_{ds} . \quad (\text{B.29})$$

Again, there are relations between these operators: equations of motion can be used to eliminate 33, 36 and 40 [60]. For  $N_f = N_v$  the contributions from the QCD and weak  $\text{O}(p^4)$ -constants to Eq. (B.5) read

$$\begin{aligned} \mathcal{E}_8(x_0, y_0) = & 8M^4 P'(x_0) P'(y_0) \left[ -E_1 - \frac{N_f}{2} E_2 + E_3 + 4E_{33} - 4E_{39} - 4E_{40} \right] + \\ & + 8M^6 P(x_0) P(y_0) \left[ E_{10} + \frac{1}{2} E_{11} + \frac{N_f}{2} E_{14} - 2E_{35} - 2E_{36} \right] + \\ & + 4M^6 P(x_0) P(y_0) g_8 F^2 [-N_f L_4 - L_5] + \\ & + 4M^6 \frac{d}{dM^2} \left[ P'(x_0) P'(y_0) \right] g'_8 F^2 \left[ -N_f L_4 - L_5 + 2(N_f L_6 + L_8) \right] . \quad (\text{B.30}) \end{aligned}$$

The results for the divergent parts of  $E_i$  can be found in Ref. [60] for  $N_f = 3$  and will be given below for general  $N_f$ . Taking into account that (in the unquenched case)

$$N_f L_4 + L_5 - 2(N_f L_6 + L_8) = N_f L_4^r + L_5^r - 2(N_f L_6^r + L_8^r) + \frac{\lambda}{4N_f} , \quad (\text{B.31})$$

where  $L_6^r, L_8^r$  are finite, and summing together with the divergences shown in Eqs. (5.9) and (5.15), it can be verified that  $\mathcal{C}_8$  is finite.

### Appendix C. The case $N_f \neq N_v$

For  $N_f \neq N_v$ , the set of possible operators is in general larger than for  $N_f = N_v$ : the only restrictions are that the operators be singlets in the full group  $\text{SU}(N_f)_R$ , and have the correct transformation properties in the subgroup  $\text{SU}(N_v)_L$ . At  $\text{O}(p^2)$  this does not change the situation for the 27-plet, but it increases the amount of octets to four in total. Besides  $\mathcal{O}_8$  defined by Eqs. (2.13), (2.12), (2.8), *viz.*

$$\mathcal{O}_8 = \frac{F^4}{8} \left[ (\mathcal{L}_\mu P_v \mathcal{L}_\mu)_{ds} + (\mathcal{L}_\mu)_{ds} \text{Tr}(P_v \mathcal{L}_\mu) \right] , \quad (\text{C.1})$$

and  $\mathcal{O}'_8$  defined by Eq. (2.14), there are two additional octets, which we choose to define such that they vanish in the limit  $N_f \rightarrow N_v$ :

$$\hat{\mathcal{O}}_8 \equiv \frac{F^4}{8} [\mathcal{L}_\mu (1 - P_v) \mathcal{L}_\mu]_{ds}, \quad (\text{C.2})$$

$$\check{\mathcal{O}}_8 \equiv \frac{F^4}{8} (\mathcal{L}_\mu)_{ds} \text{Tr} [(1 - P_v) \mathcal{L}_\mu]. \quad (\text{C.3})$$

It should also be noted that these operators only contribute starting at the NLO, since at tree-level they do not couple to two valence-flavoured mesons. Since for  $\mathcal{C}_{27}$  nothing changes with respect to Appendix B, we concentrate on the octets in the following.

The three-point octet correlation function is now of the form

$$[\mathcal{C}_8]^{ab} \equiv \int d^3x \int d^3y \left\langle \mathcal{J}_0^a(x) \left[ g_8 \mathcal{O}_8 + g'_8 \mathcal{O}'_8 + \hat{g}_8 \hat{\mathcal{O}}_8 + \check{g}_8 \check{\mathcal{O}}_8 + \sum_i E_i \bar{\mathcal{O}}_8^{(i)} \right] (0) \mathcal{J}_0^b(y) \right\rangle \quad (\text{C.4})$$

$$= \Delta_8^{ab} \left\{ g_8 \left[ \mathcal{C}(x_0) \mathcal{C}(y_0) + \mathcal{D}_8(x_0, y_0) \right] + g'_8 \mathcal{D}'_8 + \hat{g}_8 \hat{\mathcal{D}}_8 + \check{g}_8 \check{\mathcal{D}}_8 + \mathcal{E}_8 \right\}, \quad (\text{C.5})$$

where  $\mathcal{D}_8$  can be found in Eq. (5.5) and  $\mathcal{D}'_8$  in Eq. (5.14). The new functions read

$$\hat{\mathcal{D}}_8(x_0, y_0) = (N_f - N_v) \left[ -\frac{1}{2} \mathcal{D}_{27}(x_0, y_0) + \frac{F^2 M^2}{8} \mathcal{I}_A(x_0, y_0) \right], \quad (\text{C.6})$$

$$\check{\mathcal{D}}_8(x_0, y_0) = \frac{F^2 M^2}{4} \left[ N_v \mathcal{I}_B(x_0, y_0) - \mathcal{I}_A(x_0, y_0) \right], \quad (\text{C.7})$$

where we have defined

$$\begin{aligned} \mathcal{I}_A(x_0, y_0) \equiv & G(0; M^2) P'(x_0) P'(y_0) - \\ & - \frac{M^2}{2} P(x_0 - y_0) [B(x_0) + B(y_0)] + \\ & + \frac{1}{2} P'(x_0 - y_0) [B'(x_0) - B'(y_0)] + \\ & + M^4 \int_0^T d\tau B(\tau) P(\tau - x_0) P(\tau - y_0), \end{aligned} \quad (\text{C.8})$$

$$\begin{aligned} \mathcal{I}_B(x_0, y_0) \equiv & E(0; M^2) P'(x_0) P'(y_0) - \\ & - \frac{M^2}{2} P(x_0 - y_0) [\tilde{B}(x_0) + \tilde{B}(y_0)] + \\ & + \frac{1}{2} P'(x_0 - y_0) [\tilde{B}'(x_0) + \tilde{B}_0(x_0) - \tilde{B}'(y_0) - \tilde{B}_0(y_0)] + \\ & + M^2 \int_0^T d\tau \left[ M^2 \tilde{B}(\tau) + \frac{1}{2} \tilde{B}_{00}(\tau) \right] P(\tau - x_0) P(\tau - y_0), \end{aligned} \quad (\text{C.9})$$

and the notation follows that in Eq. (5.5). The divergent parts read (in the unquenched case)

$$\hat{\mathcal{D}}_8(x_0, y_0) = \hat{\mathcal{D}}_8^r(x_0, y_0) + \frac{F^2 \lambda}{4} (N_f - N_v) \left[ M^6 P(x_0) P(y_0) \right], \quad (\text{C.10})$$

$$\check{\mathcal{D}}_8(x_0, y_0) = \check{\mathcal{D}}_8^r(x_0, y_0) + \frac{F^2 \lambda}{2} \left( 1 - \frac{N_v}{N_f} \right) \left[ M^6 P(x_0) P(y_0) - M^4 P'(x_0) P'(y_0) \right], \quad (\text{C.11})$$

where  $\hat{\mathcal{D}}_8^r, \check{\mathcal{D}}_8^r$  are finite.

The list of operators contributing to  $\mathcal{E}_8$  for  $N_f \neq N_v$  is also much longer. We will not provide any systematic classification of all the possibilities, but only list the additional operators that are needed for cancelling the ultraviolet divergences at NLO. Using the same notation as in Appendix A [ $\text{Tr}_v(\dots) \equiv \text{Tr}(P_v \dots)$ ], we need

$$\bar{\mathcal{O}}_8^{(1')} \equiv -(\mathcal{S}P_v\mathcal{S})_{ds}, \quad (\text{C.12})$$

$$\bar{\mathcal{O}}_8^{(2')} \equiv -(\mathcal{S})_{ds}\text{Tr}_v(\mathcal{S}), \quad (\text{C.13})$$

$$\bar{\mathcal{O}}_8^{(10')} \equiv \{\mathcal{S}, \mathcal{L}_\mu P_v \mathcal{L}_\mu\}_{ds}, \quad (\text{C.14})$$

$$\bar{\mathcal{O}}_8^{(10'')} \equiv (\mathcal{S}P_v \mathcal{L}_\mu \mathcal{L}_\mu + \mathcal{L}_\mu \mathcal{L}_\mu P_v \mathcal{S})_{ds}, \quad (\text{C.15})$$

$$\bar{\mathcal{O}}_8^{(11')} \equiv \frac{1}{2}(\mathcal{L}_\mu \{P_v, \mathcal{S}\} \mathcal{L}_\mu)_{ds}, \quad (\text{C.16})$$

$$\bar{\mathcal{O}}_8^{(14')} \equiv (\mathcal{L}_\mu P_v \mathcal{L}_\mu)_{ds} \text{Tr}(\mathcal{S}), \quad (\text{C.17})$$

$$\bar{\mathcal{O}}_8^{(14'')} \equiv (\mathcal{L}_\mu \mathcal{L}_\mu)_{ds} \text{Tr}_v(\mathcal{S}), \quad (\text{C.18})$$

$$\bar{\mathcal{O}}_8^{(35')} \equiv -(\mathcal{L}_\mu P_v \partial_\nu \mathcal{W}_{\mu\nu} + \partial_\nu \mathcal{W}_{\mu\nu} P_v \mathcal{L}_\mu)_{ds}, \quad (\text{C.19})$$

$$\bar{\mathcal{O}}_8^{(39')} \equiv -(\mathcal{W}_{\mu\nu} P_v \mathcal{W}_{\mu\nu})_{ds}. \quad (\text{C.20})$$

With these definitions, we get:

$$\begin{aligned} \mathcal{E}_8(x_0, y_0) = & 8M^4 P'(x_0) P'(y_0) \left[ -E_1 - E_{1'} - \frac{N_f}{2} E_2 - \frac{N_v}{2} E_{2'} + E_3 + \right. \\ & \left. + 4E_{33} - 4(E_{39} + E_{39'}) - 4E_{40} \right] + \\ & + 8M^6 P(x_0) P(y_0) \left[ E_{10} + E_{10'} + E_{10''} + \frac{1}{2}(E_{11} + E_{11'}) + \right. \\ & \left. + \frac{N_f}{2}(E_{14} + E_{14'}) + \frac{N_v}{2} E_{14''} - 2(E_{35} + E_{35'}) - 2E_{36} \right] + \\ & + 4M^6 P(x_0) P(y_0) g_8 F^2 [-N_f L_4 - L_5] + \\ & + 4M^6 \frac{d}{dM^2} \left[ P'(x_0) P'(y_0) \right] g'_8 F^2 \left[ -N_f L_4 - L_5 + 2(N_f L_6 + L_8) \right]. \quad (\text{C.21}) \end{aligned}$$

Like for  $\mathcal{C}_{27}$ , the part  $\mathcal{C}(x_0)\mathcal{C}(y_0)$  in Eq. (C.5) is finite, while the other parts contain divergences. More precisely,  $\mathcal{D}_8, \mathcal{D}'_8, \hat{\mathcal{D}}_8, \check{\mathcal{D}}_8$  are of the forms shown in Eqs. (5.9), (5.15), (C.10), (C.11), the combination  $N_f L_4 + L_5$  of the form in Eq. (B.17), while the combination on the last line of Eq. (C.21) is of the form in Eq. (B.31). Moreover, writing

$$E_i = E_i^r + \frac{F^2 \lambda}{2} \left( g_8 \eta_i + g'_8 \eta'_i + \hat{g}_8 \hat{\eta}_i + \check{g}_8 \check{\eta}_i \right) \quad (\text{C.22})$$

where  $E_i^r$  are finite, the coefficients  $\eta_i, \eta'_i, \hat{\eta}_i, \check{\eta}_i$  can be derived with the method of Ref. [60]; they are listed in Table 1. Summing together, all the divergences cancel in  $\mathcal{C}_8$ , as they should.

$i$	$\eta_i$	$\eta'_i$	$\hat{\eta}_i$	$\check{\eta}_i$
1	$(N_v + 2) \left( \frac{1}{16} - \frac{1}{4N_f} \right)$	$-\frac{N_f}{4} + \frac{1}{N_f}$	$\frac{N_f - N_v}{16} - \frac{1}{4N_f}$	$-\frac{1}{8} + \frac{N_v}{4N_f}$
1'	$\frac{1}{8} - \frac{1}{4N_f}$	0	$\frac{1}{4N_f}$	$-\frac{1}{8}$
2	$(N_v + 2) \frac{1}{4N_f^2}$	$-\frac{1}{4} - \frac{1}{2N_f^2}$	$\frac{1}{8}$	$-\frac{N_v}{4N_f^2}$
2'	$\frac{1}{8} - \frac{1}{4N_f}$	0	$-\frac{1}{8}$	$\frac{1}{4N_f}$
3	0	0	0	0
10	$(N_v + 2) \left( -\frac{1}{32} + \frac{1}{16N_f} \right)$	$\frac{N_f}{8}$	$\frac{N_f + N_v}{32}$	$\frac{1}{16} \left( 1 - \frac{N_v}{N_f} \right)$
10'	$\frac{3}{16} + \frac{N_f}{16}$	0	$-\frac{N_f}{16}$	$-\frac{3}{16}$
10''	$-\frac{3}{16}$	0	0	$\frac{3}{16}$
11	$(N_v + 2) \left( -\frac{3}{8N_f} \right)$	0	$\frac{N_f}{8}$	$\frac{3N_v}{8N_f}$
11'	$\frac{3}{8} + \frac{N_f}{8}$	0	$-\frac{N_f}{8}$	$-\frac{3}{8}$
14	0	0	$\frac{1}{16}$	0
14'	$\frac{1}{4}$	0	$-\frac{1}{4}$	0
14''	$-\frac{3}{16}$	0	$\frac{3}{16}$	0
33	$(N_v + 2) \left( \frac{1}{64} - \frac{1}{32N_f} \right)$	0	$\frac{N_f - N_v}{64}$	$-\frac{1}{32} \left( 1 - \frac{N_v}{N_f} \right)$
35	$(N_v + 2) \left( -\frac{1}{32} \right)$	0	$\frac{N_v - N_f}{32}$	$\frac{1}{16}$
35'	$\frac{1}{16}$	0	0	$-\frac{1}{16}$
36	0	0	0	0
39	$(N_v + 2) \left( -\frac{1}{64} \right)$	0	$\frac{N_v - N_f}{64}$	$\frac{1}{32}$
39'	$\frac{1}{32}$	0	0	$-\frac{1}{32}$
40	0	0	0	0

Table 1: The coefficients that appear in Eq. (C.22), in the unquenched case.

The results for  $E_i$  that need to be used for the case  $N_f = N_v$  can be obtained from Table 1 by summing together the coefficients with the same “numerical” index that then correspond to the coefficients of the operators in Eqs. (B.19)–(B.29):  $(E_1 + E_{1'})_{N_f=N_v}$  for Eq. (B.19),  $(E_2 + E_{2'})_{N_f=N_v}$  for Eq. (B.20), etc. It can immediately be seen that the divergent parts proportional to  $\hat{g}_8$  and  $\check{g}_8$  cancel in these sums, as has to be the case.

We finally comment on the quenched limit, corresponding formally to  $N_f \rightarrow 0$  but  $N_v$  fixed. We have seen that for  $N_f \neq N_v$  additional operators in general appear, as elaborated in Ref. [32]. However, it is easy to see that the functions  $\mathcal{I}_A$ ,  $\mathcal{I}_B$  that appear in Eqs. (C.6), (C.7), vanish in the  $\epsilon$ -regime. Therefore the coefficient  $\check{g}_8$  does not contribute in Eq. (C.5) in the  $\epsilon$ -regime. Moreover,  $\hat{\mathcal{D}}_8$  is determined by the same function  $\mathcal{D}_{27}$  that appears in  $\mathcal{D}_8$  (cf. Eqs. (5.5), (C.6)). In particular, the normalised three-point function defined in analogy with

Eq. (5.10) obtains for  $N_f \rightarrow 0$  the form

$$\Delta_8^{ab} \left[ g_8 - (g_8 - \hat{g}_8) \frac{N_v}{(FL)^2} \left( \rho^{-\frac{1}{2}} \beta_1 - \rho k_{00} \right) \right] + g'_8 [\mathcal{C}'_8]_{\text{norm}}^{ab}(x_0, y_0). \quad (\text{C.23})$$

We observe that quenched functional behaviour only appears in the part  $[\mathcal{C}'_8]_{\text{norm}}^{ab}(x_0, y_0)$  (cf. Eq. (5.23)), and can thus be eliminated by disentangling the contributions related to  $g'_8$ , just like in Sec. 5.2. Moreover, it can be verified that at the NLO in the  $\epsilon$ -regime, the coefficients  $\hat{g}_8, \check{g}_8$  do not contribute to the correlation function considered in Sec. 5.3, such that  $g'_8$  can be separately determined just like there. The remaining terms in Eq. (C.23) allow then in principle to determine the “physical” coefficient  $g_8$ , by monitoring the volume dependence.

## Appendix D. Correlation functions for $N_v = 4$

It has been argued recently that many of the mysteries related to the  $\Delta I = 1/2$  rule can be studied particularly cleanly [both from the conceptual and from the practical point of view] by considering the SU(4) symmetric situation, i.e.  $N_v = N_f = 4$  [20]. We discuss here how our predictions can be converted to apply to that situation.

Rather than 27, 8, the dimensions of the relevant irreducible representations are 84, 20 for  $N_v = 4$ . The corresponding operators are obtained like the 27 for  $N_v = 3$ , but by using the projection operators  $P_2^\sigma P_1^\sigma$  in Eq. (A.4), with  $\sigma = +1$  for the 84 and  $\sigma = -1$  for the 20. Following the notation in Ref. [20], the corresponding operators are denoted by  $[\hat{\mathcal{O}}_1]_{rsuv}^\sigma$ .

The three-point correlation function we are interested in now takes the form

$$[\hat{\mathcal{C}}_1]_{rsuv}^{ab,\sigma}(x_0, y_0) \equiv \int d^3x \int d^3y \left\langle \mathcal{J}_0^a(x) \left\{ g_1^\sigma [\hat{\mathcal{O}}_1]_{rsuv}^\sigma(0) + \sum_i D_i^\sigma [\hat{\mathcal{O}}_i]_{rsuv}^\sigma(0) \right\} \mathcal{J}_0^b(y) \right\rangle. \quad (\text{D.1})$$

The  $\text{O}(p^4)$  weak operators  $\hat{\mathcal{O}}_i$  here have the same chiral structures as the 27-plets of Ref. [60], listed in Eqs. (B.6)–(B.13) of Appendix B, but each of them comes in two variants after the valence flavour projection, corresponding to  $\sigma = \pm$ . The result can be written in the form

$$[\hat{\mathcal{C}}_1]_{rsuv}^{ab,\sigma}(x_0, y_0) = \hat{\Delta}_{rsuv}^{ab,\sigma} \left\{ g_1^\sigma \left[ \mathcal{C}(x_0) \mathcal{C}(y_0) + \sigma \mathcal{D}_{27}(x_0, y_0) \right] + \mathcal{E}^\sigma(x_0, y_0) \right\}, \quad (\text{D.2})$$

where  $\hat{\Delta}_{rsuv}^{ab,\sigma} \equiv 2S_{rsuv}^\sigma(T^a, T^b)$ , with the function  $S_{rsuv}^\sigma(T^a, T^b)$  given in Eq. (A.14). The function  $\mathcal{D}_{27}(x_0, y_0)$  is identical to the one for the 27-plet in Eq. (4.6).

The functions  $\mathcal{E}^\sigma(x_0, y_0)$  in Eq. (D.2) contain the contributions of the  $\text{O}(p^4)$  low-energy constants, beyond those already contained in the factorized term  $\mathcal{C}(x_0) \mathcal{C}(y_0)$ :

$$\begin{aligned} \mathcal{E}^\sigma(x_0, y_0) &= 4M^4 P'(x_0) P'(y_0) [D_2^\sigma + 2D_{19}^\sigma - 4D_{24}^\sigma - 4D_{25}^\sigma] + \\ &+ 4M^6 P(x_0) P(y_0) \left[ D_4^\sigma + \frac{N_f}{2} D_7^\sigma - D_{20}^\sigma - D_{21}^\sigma - F^2(N_f L_4 + L_5) \right]. \end{aligned} \quad (\text{D.3})$$

Taking into account that  $\mathcal{C}(x_0)$  is finite, that the  $\mathcal{D}_{27}$  contains the divergences in Eq. (4.8), that the QCD  $\mathcal{O}(p^4)$  constants contain the divergence in Eq. (B.17), and that the weak  $\mathcal{O}(p^4)$  constants contain the divergences

$$D_4^\sigma = D_4^r + g_1^\sigma F^2 \lambda \left( \frac{N_f + 3\sigma}{8} \right), \quad (\text{D.4})$$

$$D_7^\sigma = D_7^r + g_1^\sigma F^2 \lambda \left( \frac{1}{4} \right), \quad (\text{D.5})$$

$$D_{20}^\sigma = D_{20}^r + g_1^\sigma F^2 \lambda \left( \frac{\sigma}{8} \right), \quad (\text{D.6})$$

$$D_{24}^\sigma = D_{24}^r + g_1^\sigma F^2 \lambda \left( \frac{\sigma}{32} \right), \quad (\text{D.7})$$

the correlation function  $\hat{\mathcal{C}}_1$  in Eq. (D.2) can be seen to be finite.

## References

- [1] M.K. Gaillard and B.W. Lee, Phys. Rev. Lett. 33 (1974) 108; G. Altarelli and L. Maiani, Phys. Lett. B 52 (1974) 351.
- [2] N. Cabibbo, G. Martinelli and R. Petronzio, Nucl. Phys. B 244 (1984) 381; R.C. Brower, G. Maturana, M.B. Gavela and R. Gupta, Phys. Rev. Lett. 53 (1984) 1318.
- [3] C.W. Bernard, T. Draper, A. Soni, H.D. Politzer and M.B. Wise, Phys. Rev. D 32 (1985) 2343.
- [4] R.J. Crewther, Nucl. Phys. B 264 (1986) 277.
- [5] A. Pich, B. Guberina and E. de Rafael, Nucl. Phys. B 277 (1986) 197; A. Pich and E. de Rafael, Nucl. Phys. B 358 (1991) 311.
- [6] J. Gasser and U.G. Meissner, Phys. Lett. B 258 (1991) 219.
- [7] J. Kambor, J. Missimer and D. Wyler, Phys. Lett. B 261 (1991) 496; J. Kambor, J.F. Donoghue, B.R. Holstein, J. Missimer and D. Wyler, Phys. Rev. Lett. 68 (1992) 1818; J. Bijnens, E. Pallante and J. Prades, Nucl. Phys. B 521 (1998) 305 [hep-ph/9801326]; E. Pallante, JHEP 01 (1999) 012 [hep-lat/9808018].
- [8] E. Pallante and A. Pich, Phys. Rev. Lett. 84 (2000) 2568 [hep-ph/9911233]; Nucl. Phys. B 592 (2001) 294 [hep-ph/0007208].
- [9] J. Gasser and H. Leutwyler, Phys. Lett. B 188 (1987) 477; Nucl. Phys. B 307 (1988) 763.
- [10] H. Neuberger, Phys. Rev. Lett. 60 (1988) 889; Nucl. Phys. B 300 (1988) 180.

- [11] P.H. Damgaard, R.G. Edwards, U.M. Heller and R. Narayanan, Phys. Rev. D 61 (2000) 094503 [hep-lat/9907016]; P. Hernández, K. Jansen and L. Lellouch, Phys. Lett. B 469 (1999) 198 [hep-lat/9907022]; P. Hernández, K. Jansen, L. Lellouch and H. Wittig, JHEP 07 (2001) 018 [hep-lat/0106011]; T. DeGrand [MILC Collaboration], Phys. Rev. D 64 (2001) 117501 [hep-lat/0107014]; P. Hasenfratz, S. Hauswirth, K. Holland, T. Jörg and F. Niedermayer, Nucl. Phys. B (Proc. Suppl.) 106 (2002) 751 [hep-lat/0109007].
- [12] S. Prelovsek and K. Orginos [RBC Collaboration], Nucl. Phys. B (Proc. Suppl.) 119 (2003) 822 [hep-lat/0209132]; W. Bietenholz, K. Jansen and S. Shcheredin, JHEP 07 (2003) 033 [hep-lat/0306022]; L. Del Debbio and C. Pica, JHEP 02 (2004) 003 [hep-lat/0309145]; L. Giusti, M. Lüscher, P. Weisz and H. Wittig, JHEP 11 (2003) 023 [hep-lat/0309189]; W. Bietenholz, T. Chiarappa, K. Jansen, K.I. Nagai and S. Shcheredin, JHEP 02 (2004) 023 [hep-lat/0311012].
- [13] P.H. Damgaard, M.C. Diamantini, P. Hernández and K. Jansen, Nucl. Phys. B 629 (2002) 445 [hep-lat/0112016].
- [14] P.H. Damgaard, P. Hernández, K. Jansen, M. Laine and L. Lellouch, Nucl. Phys. B 656 (2003) 226 [hep-lat/0211020].
- [15] L. Giusti, C. Hoelbling, M. Lüscher and H. Wittig, Comput. Phys. Commun. 153 (2003) 31 [hep-lat/0212012].
- [16] L. Giusti, P. Hernández, M. Laine, P. Weisz and H. Wittig, JHEP 01 (2004) 003 [hep-lat/0312012].
- [17] L. Giusti, P. Hernández, M. Laine, P. Weisz and H. Wittig, JHEP 04 (2004) 013 [hep-lat/0402002].
- [18] L. Del Debbio, L. Giusti and C. Pica, Phys. Rev. Lett. 94 (2005) 032003 [hep-th/0407052]; H. Fukaya, S. Hashimoto and K. Ogawa, Prog. Theor. Phys. 114 (2005) 451 [hep-lat/0504018]; T. Mehen and B.C. Tiburzi, Phys. Rev. D 72 (2005) 014501 [hep-lat/0505014]; K. Ogawa and S. Hashimoto, Prog. Theor. Phys. 114 (2005) 609 [hep-lat/0505017]; P.H. Damgaard, U.M. Heller, K. Splittorff and B. Svetitsky, Phys. Rev. D 72 (2005) 091501 [hep-lat/0508029]; P.H. Damgaard, U.M. Heller, K. Splittorff, B. Svetitsky and D. Toublan, Phys. Rev. D 73 (2006) 074023 [hep-lat/0602030]; W. Bietenholz and S. Shcheredin, hep-lat/0605013; M. Luz, hep-lat/0607022.
- [19] P. Hernández and M. Laine, JHEP 01 (2003) 063 [hep-lat/0212014].
- [20] L. Giusti, P. Hernández, M. Laine, P. Weisz and H. Wittig, JHEP 11 (2004) 016 [hep-lat/0407007].

- [21] W. Detmold and M.J. Savage, Phys. Lett. B 599 (2004) 32 [hep-lat/0407008]; P.F. Be daque, H.W. Griesshammer and G. Rupak, Phys. Rev. D 71 (2005) 054015 [hep-lat/0407009]; W. Detmold and C.-J.D. Lin, Phys. Rev. D 71 (2005) 054510 [hep-lat/0501007].
- [22] P.H. Ginsparg and K.G. Wilson, Phys. Rev. D 25 (1982) 2649.
- [23] D.B. Kaplan, Phys. Lett. B 288 (1992) 342 [hep-lat/9206013].
- [24] Y. Shamir, Nucl. Phys. B 406 (1993) 90 [hep-lat/9303005]; V. Furman and Y. Shamir, Nucl. Phys. B 439 (1995) 54 [hep-lat/9405004].
- [25] R. Narayanan and H. Neuberger, Nucl. Phys. B 412 (1994) 574 [hep-lat/9307006]; Nucl. Phys. B 443 (1995) 305 [hep-th/9411108].
- [26] H. Neuberger, Phys. Lett. B 417 (1998) 141 [hep-lat/9707022]; *ibid.* 427 (1998) 353 [hep-lat/9801031]; Phys. Rev. D 57 (1998) 5417 [hep-lat/9710089].
- [27] P. Hasenfratz, Nucl. Phys. B 525 (1998) 401 [hep-lat/9802007].
- [28] M. Lüscher, Phys. Lett. B 428 (1998) 342 [hep-lat/9802011].
- [29] Y. Kikukawa and T. Noguchi, hep-lat/9902022.
- [30] L. Giusti, P. Hernández, M. Laine, C. Pena, J. Wennekers and H. Wittig, hep-ph/0607220.
- [31] P. Hernández and M. Laine, JHEP 09 (2004) 018 [hep-ph/0407086].
- [32] M. Golterman and E. Pallante, JHEP 10 (2001) 037 [hep-lat/0108010]; Phys. Rev. D 69 (2004) 074503 [hep-lat/0212008]; hep-lat/0602025.
- [33] O. Bär, G. Rupak and N. Shores, Phys. Rev. D 67 (2003) 114505 [hep-lat/0210050]; M. Golterman, T. Izubuchi and Y. Shamir, Phys. Rev. D 71 (2005) 114508 [hep-lat/0504013].
- [34] A. Hasenfratz, P. Hasenfratz and F. Niedermayer, Phys. Rev. D 72 (2005) 114508 [hep-lat/0506024]; H. Fukaya, S. Hashimoto, K.I. Ishikawa, T. Kaneko, H. Matsufuru, T. Onogi and N. Yamada [JLQCD Collaboration], hep-lat/0607020.
- [35] C. Pena, S. Sint and A. Vladikas, JHEP 09 (2004) 069 [hep-lat/0405028]; R. Frezzotti and G.C. Rossi, JHEP 10 (2004) 070 [hep-lat/0407002]; P. Boucaud, V. Giménez, C.-J.D. Lin, V. Lubicz, G. Martinelli, M. Papinutto and C.T. Sachrajda, Nucl. Phys. B 721 (2005) 175 [hep-lat/0412029]; P. Dimopoulos, J. Heitger, F. Palombi, C. Pena, S. Sint and A. Vladikas [ALPHA Collaboration], hep-ph/0601002.

- [36] W.A. Bardeen, A.J. Buras and J.-M. Gérard, Phys. Lett. B 180 (1986) 133; Nucl. Phys. B 293 (1987) 787; Phys. Lett. B 192 (1987) 138.
- [37] T. Hambye, S. Peris and E. de Rafael, JHEP 05 (2003) 027 [hep-ph/0305104]; J. Bijnens, E. Gamiz and J. Prades, JHEP 03 (2006) 048 [hep-ph/0601197].
- [38] H. Georgi, *Weak Interactions and Modern Particle Theory* (Benjamin/Cummings, Menlo Park, California, 1984); J.F. Donoghue, E. Golowich and B.R. Holstein, *Dynamics of the Standard Model* (Cambridge University Press, Cambridge, 1992).
- [39] A. Pich, Rept. Prog. Phys. 58 (1995) 563 [hep-ph/9502366]; G. Ecker, Prog. Part. Nucl. Phys. 36 (1996) 71 [hep-ph/9511412].
- [40] G. Altarelli, G. Curci, G. Martinelli and S. Petrarca, Nucl. Phys. B 187 (1981) 461; A.J. Buras and P.H. Weisz, Nucl. Phys. B 333 (1990) 66.
- [41] A.I. Vainshtein, V.I. Zakharov and M.A. Shifman, JETP Lett. 22 (1975) 55; M.A. Shifman, A.I. Vainshtein and V.I. Zakharov, Nucl. Phys. B 120 (1977) 316.
- [42] F.J. Gilman and M.B. Wise, Phys. Rev. D 20 (1979) 2392.
- [43] J. Gasser and H. Leutwyler, Annals Phys. 158 (1984) 142; Nucl. Phys. B 250 (1985) 465.
- [44] J.A. Cronin, Phys. Rev. 161 (1967) 1483.
- [45] H. Leutwyler, Phys. Lett. B 189 (1987) 197.
- [46] P.H. Damgaard and K. Splittorff, Phys. Rev. D 62 (2000) 054509 [hep-lat/0003017].
- [47] P. Hasenfratz and H. Leutwyler, Nucl. Phys. B 343 (1990) 241.
- [48] H. Leutwyler and A. Smilga, Phys. Rev. D 46 (1992) 5607.
- [49] F.C. Hansen, Nucl. Phys. B 345 (1990) 685; F.C. Hansen and H. Leutwyler, Nucl. Phys. B 350 (1991) 201.
- [50] R. Brower, P. Rossi and C.I. Tan, Nucl. Phys. B 190 (1981) 699.
- [51] M.F.L. Golterman and K.C. Leung, Phys. Rev. D 56 (1997) 2950 [hep-lat/9702015]; C.-J.D. Lin, G. Martinelli, E. Pallante, C.T. Sachrajda and G. Villadoro, Nucl. Phys. B 650 (2003) 301 [hep-lat/0208007].
- [52] D. Bećirevic and G. Villadoro, Phys. Rev. D 69 (2004) 054010 [hep-lat/0311028].
- [53] G. Colangelo and C. Haefeli, Phys. Lett. B 590 (2004) 258 [hep-lat/0403025]; G. Colangelo, S. Dürr and C. Haefeli, Nucl. Phys. B 721 (2005) 136 [hep-lat/0503014].

- [54] J. Laiho and A. Soni, Phys. Rev. D 65 (2002) 114020 [hep-ph/0203106]; Phys. Rev. D 71 (2005) 014021 [hep-lat/0306035].
- [55] C.W. Bernard and M.F.L. Golterman, Phys. Rev. D 46 (1992) 853 [hep-lat/9204007].
- [56] S.R. Sharpe, Phys. Rev. D 46 (1992) 3146 [hep-lat/9205020].
- [57] J.C. Osborn, D. Toublan and J.J. Verbaarschot, Nucl. Phys. B 540 (1999) 317 [hep-th/9806110]; P.H. Damgaard, J.C. Osborn, D. Toublan and J.J. Verbaarschot, Nucl. Phys. B 547 (1999) 305 [hep-th/9811212].
- [58] G. Colangelo and E. Pallante, Nucl. Phys. B 520 (1998) 433 [hep-lat/9708005].
- [59] H. Georgi, *Lie Algebras in Particle Physics* (Benjamin/Cummings, Reading, Massachusetts, 1982).
- [60] J. Kambor, J. Missimer and D. Wyler, Nucl. Phys. B 346 (1990) 17.
- [61] G. Esposito-Farèse, Z. Phys. C 50 (1991) 255; G. Ecker, J. Kambor and D. Wyler, Nucl. Phys. B 394 (1993) 101.